Arteriosclerosis, Thrombosis, and Vascular Biology

BASIC SCIENCES

Towards the Therapeutic Use of Thrombospondin 1/CD47 Targeting TAX2 Peptide as an Antithrombotic Agent

Albin Jeanne,* Thomas Sarazin,* Magalie Charlé, Charlotte Kawecki, Alexandre Kauskot, Tobias Hedtke, Christian E.H. Schmelzer, Laurent Martiny, Pascal Maurice,† Stéphane Dedieu†

OBJECTIVE: TSP-1 (thrombospondin 1) is one of the most expressed proteins in platelet α-granules and plays an important role in the regulation of hemostasis and thrombosis. Interaction of released TSP-1 with CD47 membrane receptor has been shown to regulate major events leading to thrombus formation, such as, platelet adhesion to vascular endothelium, nitric oxide/cGMP (cyclic guanosine monophosphate) signaling, platelet activation as well as aggregation. Therefore, targeting TSP-1:CD47 axis may represent a promising antithrombotic strategy.

APPROACH AND RESULTS: A CD47-derived cyclic peptide was engineered, namely TAX2, that targets TSP-1 and selectively prevents TSP-1:CD47 interaction. Here, we demonstrate for the first time that TAX2 peptide strongly decreases platelet aggregation and interaction with collagen under arterial shear conditions. TAX2 also delays time for complete thrombotic occlusion in 2 mouse models of arterial thrombosis following chemical injury, while *Thbs1*$^{-/-}$ mice recapitulate TAX2 effects. Importantly, TAX2 administration is not associated with increased bleeding risk or modification of hematologic parameters.

CONCLUSIONS: Overall, this study sheds light on the major contribution of TSP-1:CD47 interaction in platelet activation and thrombus formation while putting forward TAX2 as an innovative antithrombotic agent with high added-value.

GRAPHIC ABSTRACT: A graphic abstract is available for this article.

Key Words: cardiovascular diseases ■ CD47 antigen ■ platelet aggregation ■ thrombosis ■ thrombospondin 1

Thrombotic cardiovascular diseases, including heart attack, stroke, and peripheral vascular diseases, are the leading cause of death in developed countries.[1] Current antithrombotic drugs, including antiplatelet agents and anticoagulants, are associated with significant bleeding risk.[2,3] Platelets play an important role in hemostasis and thrombosis. At sites of vascular injury, platelets are exposed to adhesive proteins within the vascular wall and to soluble agonists, which initiates platelet adhesion, activation, transduction of intracellular signaling, granule secretion, leading to thrombus formation.[4] One of the most highly expressed proteins within platelet α-granules is the homotrimeric, multidomain glycoprotein TSP-1 (thrombospondin 1), which is rapidly released in large amounts during platelet activation.[5] While TSP-1 circulates at very low concentrations in plasma (0.1–0.3 µg/mL),[6] secretion from α-granules upon platelet activation increases TSP-1 plasma concentrations up to 100-fold.[7] Accumulating data from the literature have shown that TSP-1 plays a major role in regulating platelet activation and stable thrombus formation. TSP-1 interacts with several platelet receptors including integrin $\alpha_{IIb}\beta_3$, also known as GP (glycoprotein) IIb/IIIa,[8] GP Ib-V-IX

Correspondence to: Dr Pascal Maurice, UMR CNRS/URCA 7369 MEDyC, UFR Sciences Exactes et Naturelles, Moulin de la Housse, BP1039, 51687 Reims cedex 2, France, Email pascal.maurice@univ-reims.fr; or Pr Stéphane Dedieu, UMR CNRS/URCA 7369 MEDyC, UFR Sciences Exactes et Naturelles, Moulin de la Housse, BP1039, 51687 Reims cedex 2, France, Email stephane.dedieu@univ-reims.fr

*These authors contributed equally to this article as co-first authors.

†These authors contributed equally to this article as co-senior authors.

The Data Supplement is available with this article at https://www.ahajournals.org/doi/suppl/10.1161/ATVBAHA.120.314571.

For Sources of Funding and Disclosures, see page e15.

Arterioscler Thromb Vasc Biol is available at www.ahajournals.org/journal/atvb

Nonstandard Abbreviations and Acronyms

GP	glycoprotein
IAP	integrin-associated protein
PRP	platelet-rich plasma
TSP-1	thrombospondin 1
VWF	von Willebrand factor
WT	wild type

complex,[9] CD36,[10] and the IAP (integrin-associated protein or CD47).[11] Under arterial shear conditions, immobilized TSP-1 has been shown to mediate firm platelet adhesion via interaction with the GP Ib-V-IX complex, independently of VWF (von Willebrand factor).[9] However, conflicting evidence gathered by Prakash et al[12] indicate that platelet-derived TSP-1 requires VWF to modulate arterial thrombosis in mice. TSP-1 also protects endothelium-bound VWF from ADAMTS13 (a disintegrin and metalloprotease with a thrombospondin type 1-motif 13)-mediated degradation, thereby further enhancing the dynamic recruitment of circulating platelets within developing thrombi.[13] Besides, TSP-1 regulates platelet activation via direct interaction with either CD36 or CD47 receptors. CD47 is an atypical member of the Ig superfamily with a single extracellular domain, a unique 5 membrane-spanning domain and an alternatively spliced cytoplasmic tail.[14] This membrane receptor is activated by the globular carboxy-terminal cell-binding domain of TSP-1,[11] and TSP-1 binding to CD47 triggers activation of $\alpha_{IIb}\beta_3$ integrin, synergizes with collagen to activate platelets via $\alpha_2\beta_1$, and plays role in platelet recruitment to sites of endothelial inflammation.[15–17] Moreover, TSP-1 interaction with CD47 has been shown to negatively regulate one of the 2 major nucleotide pathways in platelets, that is, the NO-cGMP-PKG (nitric oxide-cyclic guanosine monophosphate-protein kinase G) pathway.[18] Altogether, this extensive set of data establishes the TSP-1:CD47 axis as an interesting pharmacological target for controlling platelet activation in prothrombotic diseases.

We recently engineered an innovative antagonist being selective for TSP-1:CD47 interaction, namely TAX2 peptide,[19] which exhibits promising anticancer activities in several indications.[19–21] In the present study, we evaluated TAX2 effects on platelet aggregation and thrombus formation both in vitro and in vivo, thereby demonstrating a strong antithrombotic effect of TAX2. Importantly, we also show that TAX2 administration is not associated with increased risk of bleeding nor modification of hematologic parameters. In addition to strengthen the critical role played by TSP-1:CD47 axis during platelet activation and arterial thrombosis, these results further indicate that TAX2 should be considered as a new strategy of therapeutic interest for controlling platelet activation in prothrombotic diseases while displaying a promising pharmacological safety profile.

Highlights

- The TAX2 peptide, the first-ever orthosteric antagonist of TSP-1 (thrombospondin-1):CD47 interaction, strongly decreases human platelet aggregation induced by different agonists.
- The TAX2 peptide delays time for complete thrombotic occlusion in two relevant murine models of chemically induced arterial thrombosis.
- The TAX2 peptide recapitulates the antithrombotic effects observed from TSP-1-deficient mice, hence ensuring its on-target efficacy.
- Acute or chronic TAX2 administration is safe and not associated with increased risk of bleeding nor modification of coagulation parameters.

MATERIALS AND METHODS

The data that support the findings of this study are available from the corresponding author upon reasonable request.

Peptide Synthesis

TAX2 peptide (CEVSQLLKGDAC) and the scrambled control peptide were synthesized by Genecust (Boynes, France) at a purity of 98% or higher (acetate salt as a counter-ion) and then controlled by HPLC (high-performance liquid chromatography) followed by LC-MS-MS (liquid chromatography-mass spectrometry-mass spectrometry) analysis. The scrambled peptide has been already validated and used as reference control in several publications.[19,20,22,23] Using surface plasmon resonance and microscale thermophoresis, TAX2 has been shown to bind to human[20] and mouse (data not shown) TSP-1 with comparable affinity (micromolar range). In both assays, no interaction was detected between TSP-1 and the scramble peptide.

Reagents and Antibodies

Apyrase, PGE_1, thrombin, rhodamine 6G, ferric chloride ($FeCl_3$), and NaCl 0.9% solution were purchased from Sigma-Aldrich (Saint-Quentin Fallavier, France). Lovenox was obtained from Sanofi (Paris, France). PPACK (D-phenylalanyl-L-prolyl-L-arginine chloromethylketone) and antiphosphotyrosine antibody (clone 4G10) were purchased from Merck Millipore (Darmstadt, Germany). Horm collagen was from Hyphen BioMed (Neuville-sur-Oise, France). TRAP-6 (thrombin receptor activator for peptide 6) and ADP were purchased from Roche Diagnostics (Meylan, France). Clopidogrel bisulfate was from Selleckchem (Euromedex, Souffelweyersheim, France). Anti-CD47 (clones B6H12 and MIAP301) antibodies were purchased from BD Pharmingen (Le Pont-de-Claix, France). Anti-TSP-1 (clone A6.1), anti-GPIIb (clone EPR4330), anti-GPIIIa (clone EPR2342), anti-GPIb (clone EPR6995), and anti-CD36 (clone EPR6573) antibodies were purchased from Abcam (Paris, France). Antibodies against β-actin, normal mouse and rat IgG were from Santa Cruz Biotechnology (Tebu-bio, Le Perray-en-Yvelines, France). HRP (horseradish peroxidase)-linked secondary antibodies anti-mouse IgG, anti-rat IgG, and anti-rabbit IgG were purchased from Cell Signaling Technology (Ozyme, Saint-Quentin-en-Yvelines, France). Anti-VWF and HRP-linked anti-VWF antibodies were

purchased from Dako Agilent. FITC (fluorescein isothiocyanate)-conjugated anti-mouse $GPIb_{\beta}$ (clone Xia.C3), GPVI (clone JAQ1), and α_2 (clone Sam.G4) were purchased from Emfret Analytics (Eibelstadt, Germany). FITC-conjugated anti-mouse α_{IIb} (clone MWReg30) was from BD Biosciences (Le Pont de Claix, France).

Animals

All mouse experiments were approved by the Ethics Committee for Animal Welfare of the University of Reims Champagne-Ardenne (CEEA-RCA n° 56) and the French Ministry of Research (APAFIS No. 2017112219534446 No. 13135) being compliant with the European Directive 2010/63/UE. Rat toxicity studies were approved the CEEA-75 and the French Ministry of Research (APAFIS No. 3715-2015100912474662v2). C57BL/6JRj wild-type (WT) male mice and Sprague Dawley rats were purchased from Janvier Labs (Saint-Berthevin, France). *Thbs1*$^{-/-}$ C57BL/6 (B6.129S2-Thbs1^{tm1Hyn}/J) male mice were purchased from Charles River Labs (L'Arbresle, France).

Mice Genotyping

Thbs1$^{-/-}$ and WT mice were genotyped by PCR using Phire Animal Tissue Direct PCR Kit from Thermo Scientific. Tail biopsies and blood samples were collected from anesthetized mice, and DNA was amplified by PCR using a Mastercycler nexus Flexlid thermocycler from Eppendorf AG (Hamburg, Germany). A mixture of the following primers oIMR5186: 5′-GAGTTTGCTTGTGGTGAACGCTCAG-3′ (common), oIMR5187: 5′-AGGGCTATGTGGAATTAATATCGG-3′ (WT),andoIMR5188:5′-TGCTGTCCATCTGCACGAGACTAG-3′ (mutant) was used to amplify (30 cycles of 10 seconds at 98°C, 5 seconds at 56°C, and 20 seconds at 72°C) a 400-bp and a 700-bp DNA fragments from *Thbs1*$^{-/-}$ and WT mice, respectively. The PCR fragments were then fractionated on an agarose gel prepared in TBE and containing ethidium bromide.

Blood Sample From Human Donors

Human blood was drawn from healthy donors of the Établissement Français du Sang Grand Est (EFS Grand Est, Nancy, France) who gave their informed written consent in accordance with the guidelines of the EFS Grand Est. Blood samples were collected using Vacutainer tubes containing 129 mmol/L trisodium citrate (BD Biosciences) purchased from Ozyme (Saint-Quentin-en-Yvelines, France). The study was conducted in accordance with the Declaration of Helsinki.

Whole Blood Platelet Aggregation

Whole blood aggregation was monitored by impedance aggregometry using the Multiplate analyser from Roche Diagnostics (Meylan, France). Whole blood was diluted (1:1) in NaCl 0.9% and incubated with TAX2 peptide (100 to 800 µmol/L) for 3 minutes at 37 °C before adding collagen (3.2 µg/mL), ADP (6.5 µmol/L), and TRAP-6 (32 µmol/L). Curves were recorded during at least 6 minutes, and platelet aggregation was expressed as area under the curve in arbitrary aggregation units over the time.

Platelet-Rich Plasma and Washed Platelet Aggregation

Platelet-rich plasma (PRP) was obtained by centrifugation of acid-citrate-dextrose (citric acid 130 mmol/L, Na_3-citrate 124 mmol/L, *D*-glucose 110 mmol/L) anticoagulated human whole blood for 7 minutes at 160*g* at room temperature with low acceleration and no brakes settings. Washed platelets were obtained from PRP by centrifugation for 10 minutes at 750*g* with low acceleration and no brakes settings and then washed twice with washing buffer (citric acid 36 mmol/L, glucose 5 mmol/L, KCl 5 mmol/L, $MgCl_2$ 1 mmol/L, NaCl 103 mmol/L) in presence of apyrase (0.1 IU/mL) and PGE_1 (100 nmol/L) to minimize platelet activation. Washed platelets were adjusted to 3.10^8/mL in Tyrode buffer (NaCl 137 mmol/L, KCl 2 mmol/L, NaH_2PO_4 0.3 mmol/L, $MgCl_2$ 1 mmol/L, glucose 5.5 mmol/L, HEPES 5 mmol/L, $NaHCO_3$ 12 mmol/L, $CaCl_2$ 2 mmol/L, pH 7.3). Aggregation was monitored for 3 minutes by measuring light transmission using an 8-channel Soderel aggregometer (SD Medical, France).

Protein Phosphorylation Analysis

Washed platelets were stimulated by collagen (4 µg/mL) in the cuvette of the aggregometer, and then the reaction was stopped after 6 minutes by adding Laemmli buffer. After SDS-PAGE and transfer to nitrocellulose membrane (Amersham Biosciences), membranes were probed with monoclonal antiphosphotyrosine (clone 4G10, 1:1000) or anti-β-actin (0.2 µg/mL) antibodies overnight at 4 °C, followed by HRP-linked anti-mouse IgG (1:5000) antibodies for 1 hour at room temperature. Immunoreactive bands were revealed using ECL Prime chemiluminescence detection reagents (Amersham Biosciences) and visualized using the Licor Odyssey Fc imager (Licor ScienceTec, Courtaboeuf, France).

Label-Free Quantification by Mass Spectrometry of Phosphorylated Proteins

Washed platelets were stimulated by collagen (4 µg/mL) for 3 minutes in the cuvette of the aggregometer and reaction was stopped by adding lysis buffer (NaCl 150 mmol/L, Tris-HCl 50 mmol/L, EDTA 2 mmol/L, NP-40 1%, protease inhibitor cocktail, NaF 10 mmol/L, Na_3VO_4 2 mmol/L, pH 7.5). Equal amounts of proteins were subjected to immunoprecipitation using the 4G10 antibody. After detergent-free washes, trypsin digestion of the retained proteins was directly performed on beads (27°C, 30 minutes) according to Turriziani et al.[24] Recovered peptides were then reduced by DTT, alkylated with iodoacetamide, acidified with trifluoroacetic acid, and desalted in C18 ZipTip. The peptide mixtures were analyzed on an Ultimate 3000 RSLCnano system coupled to an Orbitrap Fusion mass spectrometer equipped with a Nanospray Flex Ion Source (Thermo Fisher Scientific). Briefly, the samples were loaded on the trap column (Acclaim PepMap RP-C18, 300 µm×5 mm, 5 µm, 100 Å) and washed with water containing 0.1% FA for 15 minutes (30 µL min^{-1}), before the peptides were separated on the analytical column (Acclaim PepMap RP-C18, 75 µm×250 mm, 2 µm, 100 Å) using gradients from 1% to 35% B (90 minutes), 35% to 85% B (5 minutes) followed by 85% B (5 minutes), with solvent A: 0.1% FA in water and solvent B: 0.08% FA in acetonitrile. Data were acquired in the data-dependent MS/MS mode. Each high-resolution full-scan in the Orbitrap (*m/z* 300–1700, R=120000) was followed by high-resolution product ion

scans in the Orbitrap (collision-induced dissociation), 35% normalized collision energy, R=15 000 within 5 s, starting with the most intense signal in the full-scan mass spectrum (quadrupole isolation window 2 Th). Dynamic exclusion for 60 s (mass window±2 ppm) was enabled to allow analysis of less abundant species. Data acquisition was controlled with Xcalibur. Peptides were then identified by automated de novo sequencing followed by matching to the Swiss-Prot database using the software PEAKS Studio (version X; Bioinformatics Solutions, Waterloo, ON, Canada). The enzyme was set to trypsin and a maximum of 3 missed cleavages was allowed. Carbamidomethylation of cysteine was considered as fixed modification, phosphorylation of serine, threonine, tyrosine, and deamidation of glutamine and asparagine residues were selected as variable modifications. Mass error tolerances for precursor and fragment ions were set to 5 ppm and 0.015 Da, respectively. The peptide score threshold was decreased until a false discovery rate of ≤1% on the peptide spectrum match level was reached and a minimum of 2 unique peptides were required for protein identification. The number of spectra were used as a semiquantitative measure for selected proteins.

Co-immunoprecipitation

Human and mouse washed platelets resuspended in Tyrode buffer (3.10^8/mL) were incubated with TAX2 peptide (800 µmol/L) or the scrambled control peptide (800 µmol/L) before incubation with thrombin (0.2 IU/mL) for 5 minutes at room temperature and without stirring. Platelets were then solubilized in ice-cold lysis buffer (NaCl 150 mmol/L, HEPES 25 mmol/L, EDTA 5 mmol/L, octyl β-d-glucopyranoside 0.5%, NP-40 1%, pH 7.3) supplemented with Halt protease and phosphatase inhibitor cocktail (Thermo Fisher Scientific), NaF (10 mmol/L), Na_3VO_4 (2 mmol/L), and cantharidine (10 µmol/L). Protein concentrations were measured using the BCA Protein Assay kit (Uptima), and equal amounts of protein lysates were subjected to immunoprecipitation using the Pierce co-immunoprecipitation kit (Thermo Fisher Scientific) according to the manufacturer's protocol. Briefly, 10 µg of antibody (anti-CD47, anti-TSP-1, or nonspecific IgG) were incubated with an amine-reactive resin and covalently coupled using sodium cyanoborohydride for 2 hours at room temperature. The antibody-coupled resin was then incubated with platelet protein lysate overnight at 4°C under gentle agitation. After washings with ice-cold lysis buffer supplemented with protease inhibitors, protein complexes bound to the antibody were eluted, reduced, and separated by SDS-PAGE. Immunoblotting was performed as described above.

Platelet Interaction With Immobilized Collagen Under Arterial Shear Condition

Blood was drawn from anesthetized C57BL/6J wild type or *Thbs1*$^{-/-}$ mice vena cava using a 26 g needle mounted on 1 mL syringe containing 80 µmol/L PPACK and 10 IU/mL Lovenox. Human blood was obtained by venipuncture from consenting healthy human donors and anticoagulated with sodium citrate (0.129 mol/L) using Vacutainer tubes. Citrated human blood samples were recalcified with $MgCl_2$ 3.75 mmol/L and $CaCl_2$ 7.5 mmol/L (final concentrations) in the presence of PPACK (40 mmol/L) as previously described.[25] Murine and human whole blood (500 µL) was then incubated 10 minutes at 37°C in the dark with TAX2 peptide (100 µmol/L), the scrambled peptide (100 µmol/L), or vehicle (NaCl 0.9%) together with rhodamine 6G (10 µg/mL) to label platelets. Whole blood was then perfused over collagen-coated (50 µg/mL) perfusion chambers (Cellix Vena8 Fluoro+ Biochips, Tebu-bio, Le Perray-en-Yvelines, France) under arterial shear condition (1500 s^{-1}). Real-time thrombus formation was observed using an epifluorescence microscope (Olympus BX51WIF, Olympus France S.A.S., Rungis, France) connected to a digital camera (Olympus CAM-UC90). The percentage of surface area covered by platelets was measured over time using the ImageJ software.

Mouse Models of Chemically Induced Arterial Thrombosis

Anesthetized mice were intravenously injected with 100 µL of TAX2 peptide (10 mg/kg), scrambled control peptide (10 mg/kg), or vehicle (NaCl 0.9%). Intravenous administrations of clopidogrel (5 mg/kg) were performed 4 hours before the experiments. The mesenteric arteriole was isolated from the surrounding tissue, spread onto a microscopic glass, and rhodamine 6G (1 mg/mL) was then retro-orbitally injected.[26] Redox-induced vascular endothelial injury was achieved by applying a piece of filter paper (2×1 mm) saturated with a 10% ferric chloride ($FeCl_3$) solution directly on the mesenteric arteriole for 5 minutes. The filter paper was then removed, and thrombus formation was observed in real time as described above. The same procedure was performed on the carotid artery, except that the isolated carotid artery was placed forward of a small piece of nontransparent black plastic film to prevent fluorescence interferences by underlying structures during the visualization of blood flow.[27] In addition, the chemical injury was triggered by applying a piece of filter paper (2×1 mm) saturated with 7.5% $FeCl_3$ and placed for 1 minute. Time for complete thrombotic occlusion was defined as blood flow being stopped for at least 30 seconds.

Tail Bleeding Time

Tail bleeding times were measured on anesthetized mice intravenously injected with TAX2 peptide (10 mg/kg), scrambled control peptide (10 mg/kg), or vehicle (NaCl 0.9%). Intravenous administrations of clopidogrel (5 mg/kg) were performed 4 hours before the experiments. Tails were cut at constant diameter (1.35 mm) and then immediately immersed in a 0.9% isotonic saline buffer heated at 37°C with the tip of tail being placed 5 cm below the animal body. Bleeding was followed visually, and time to stable cessation of bleeding (ie, no rebleeding within 1 minute) was recorded.

Toxicity Studies of TAX2 Peptide in Rats and Hematologic Parameters Evaluation

Intraperitoneal injections of TAX2 peptide (100, 300, or 400 mg/kg) were performed on Sprague Dawley rats (6–8 weeks at study initiation; 5 females and 5 males per group) either one time (acute) or once daily for 7 consecutive days (repeated) for evaluation of acute and repeated dosing toxicity, respectively. Animals were monitored for 14 days including observations twice a day for morbidity, mortality, or any clinical sign, as well as body weight and food consumption measurements. Blood samples were collected from retro-orbital sinus of isoflurane

anesthetized animals into EDTA for platelet count or citrate tubes for clinical chemistry on day 2 (one day after the first dosing) and day 15 (study termination) for acute dosing toxicity, or on day 1 (prior the first dosing) and day 15 (study termination) for repeated dosing toxicity. All animals were fasted overnight on day 14 before second blood collection (day 15). Clinical chemistry included prothrombin time and activated partial thromboplastin time. Hematology analysis included: red blood corpuscles, hemoglobin, hematocrit. At study termination (day 14), animals were euthanized, and each animal underwent gross pathology evaluation of major tissue and organ systems. During necropsy, organs (heart, lungs, liver, spleen, kidneys, small and large intestines, ovaries/testes, and pancreas) from all animals were collected and wet weighed (except intestines).

VWF Antigen and VWF Multimeric Structure Analysis

Intraperitoneal injections of TAX2 peptide (100 mg/kg), or vehicle, were performed on C57BL/6J mice (8 weeks at study initiation; 5 males per group) either one time (acute) or once daily for 7 consecutive days (repeated). Blood samples were collected at day 15 from retro-orbital sinus of isoflurane anesthetized animals into heparin tubes, and plasma were recovered after centrifugation of anticoagulated whole blood (1500*g*, 20 minutes). Plasma VWF antigen (VWF:Ag) levels were quantified as described previously.[28] Briefly, rabbit polyclonal anti-VWF antibody was coated into wells of a microtiter plate in a carbonate buffer (overnight, 4 °C), washed and then blocked with BSA 3%/Tween 0.1%. Samples were then added for 2 hours at 37 °C and then washed. VWF was detected by using an anti-VWF antibody coupled to HRP and incubated during 2 hours at 37 °C. Antibody was detected by using OPD (o-phenylenediamine), and the reaction was stopped with H_2SO_4 3 mol/L and read at 492 nm. The multimeric structure of VWF was analyzed from mouse plasma by 0.1% SDS and 1.5% agarose gel electrophoresis as described previously.[29] Multimers were visualized using an alkaline phosphatase-conjugated antihuman VWF polyclonal antibody.

Flow Cytometry Analysis

Washed platelets were resuspended in Tyrode buffer at the concentration of 2.10^6/mL and incubated with anti-GPIb$_\beta$ (1:20), GPVI (1:20), α_2 (1:20), or anti-GPIIb (1:8) fluorophore-conjugated antibodies for 10 minutes in the dark at room temperature. Reaction was stopped by adding 500 µL PBS before samples were analyzed using a BD Accuri C6 flow cytometer (BD Biosciences, Le-Pont-de-Claix, France). Platelets were gated using their forward and side scatter characteristics. Acquisitions of 50 000 events were analyzed using BD CSampler software (BD Biosciences), and results were expressed as mean fluorescence intensities minus control isotype mean fluorescence intensities.

Statistical Analysis

Data were expressed as mean±SEM of at least 3 independent experiments. In vitro and ex vivo parametric data were compared using 2-tailed Student *t* test or ANOVA. In vivo nonparametric data were compared using 2-tailed Mann-Whitney-Wilcoxon *U* test or Kruskal-Wallis test. $P<0.05$ was considered to be statistically significant. Statistical analysis was performed using GraphPad Prism software version 7 (GraphPad Software, La Jolla).

RESULTS

Human Platelet Aggregation Is Decreased by TAX2 Peptide

To investigate the effect of TAX2 peptide on platelet aggregation, human whole blood was incubated in presence of increasing concentrations of either TAX2, a previously validated scrambled peptide,[19] or vehicle (NaCl 0.9%), and then aggregation was triggered by weak (ADP) and strong (collagen, TRAP-6) platelet agonists. From 100 µmol/L, TAX2 tends to decrease platelet aggregation induced by collagen, ADP, and TRAP-6 (Figure 1 and Figure I in the Data Supplement). At 400 µmol/L, whole blood platelet aggregation induced by collagen, ADP, and TRAP-6 was decreased by 36.8±6.9% (Figure 1A), 28.0±8.7% (Figure IA in the Data Supplement), and 20.8±8.0% (Figure IB in the Data Supplement), respectively, compared with the scrambled peptide. Increasing TAX2 concentration up to 800 µmol/L had no further inhibitory effect, except for ADP for which inhibition of platelet aggregation reached 54.0±11.2% (Figure IA in the Data Supplement).

The effect of TAX2 on platelet aggregation was then evaluated in PRP and washed platelets using collagen and TRAP-6 as agonists. In PRP, platelet aggregation induced by 1 µg/mL collagen or 10 µmol/L TRAP-6 was significantly decreased by 23.3±7.4% (Figure 1B) and 24.3±10.3% (Figure IC in the Data Supplement), respectively, in presence of 800 µmol/L TAX2. Below 800 µmol/L TAX2, no significant inhibitory effect was observed. However, inhibition of aggregation under TAX2 application was more potent as agonists concentration was decreased, especially for TRAP-6, for which inhibition of platelet aggregation reached 75.5±16.4% and 65.9±22.5% at 400 and 800 µmol/L, respectively, (Figure IC in the Data Supplement). The highest inhibitory effect of TAX2 was achieved in washed platelets. In this context, platelet aggregation induced by 4 µg/mL collagen and by 10 µmol/L TRAP-6 was decreased by 42.1±16.9% (Figure 1E) and 70.1±13.2% (Figure ID in the Data Supplement), respectively, in presence of 400 µmol/L TAX2. Here again, raising TAX2 concentration or decreasing the concentration of agonists further increased the inhibitory effect of TAX2. Of note, a trend for a delay of the lag phase was consistently observed under TAX2 treatment during collagen-induced platelet aggregation (Figure 1). The lag phase is defined as the delay time occurring between the addition of collagen and the onset of aggregation, during which platelets adhere to collagen fibrils and undergo shape change, and then release. This first

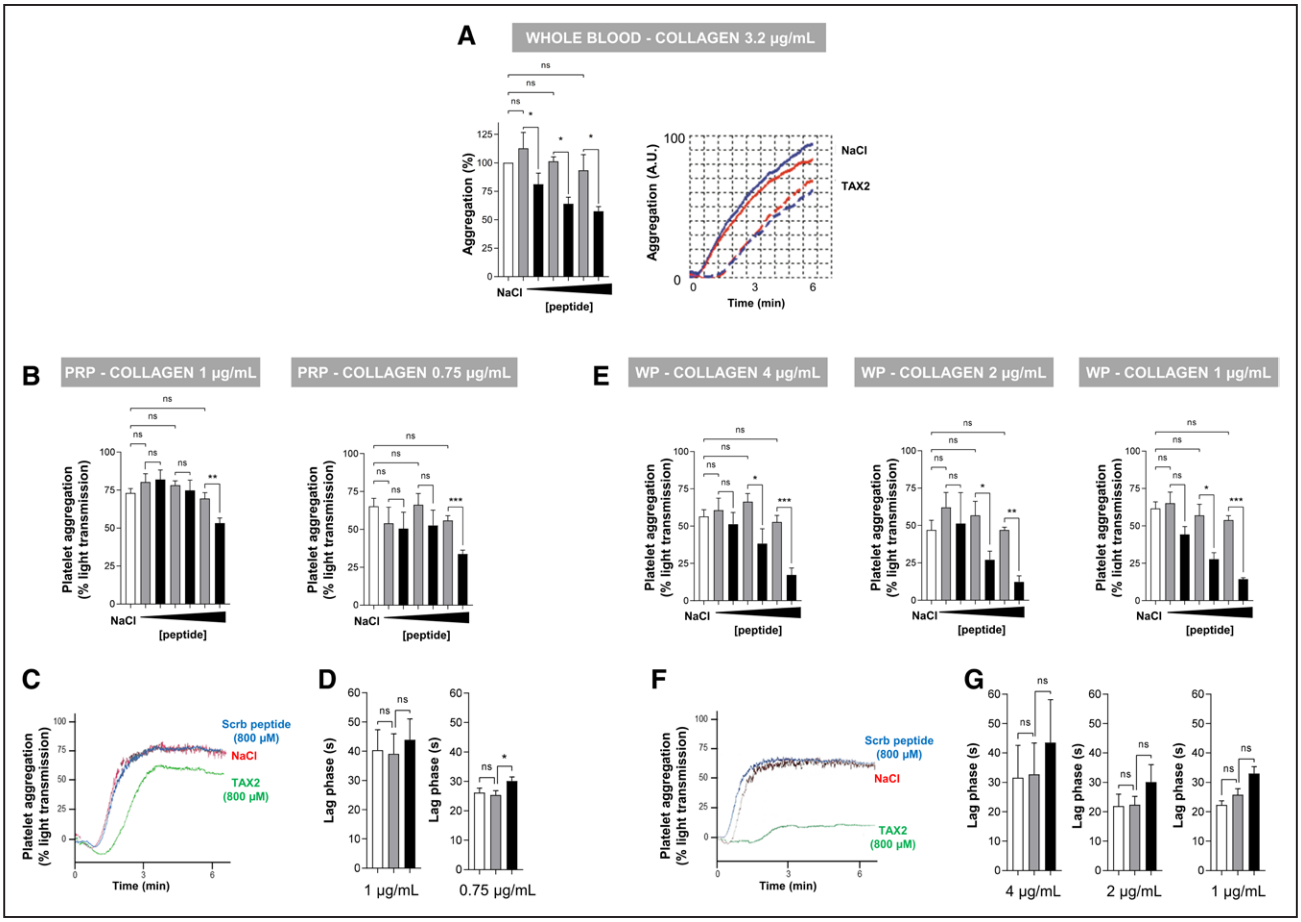

Figure 1. TAX2 peptide inhibits collagen-induced platelet aggregation in human whole blood, platelet-rich plasma, and washed platelets.

A, TAX2 or the scrambled peptide (100, 400, and 800 µmol/L) were incubated with human whole blood 3 min before addition of 3.2 µg/mL collagen, and platelet aggregation was measured by the Multiplate analyzer. **Left** graph shows the results expressed as area under the curve (AUC) of arbitrary aggregation units (AU) and normalized to the control (NaCl 0.9%). **Right** graph shows a representative aggregation curve. AUC is measured over a total time of 6 min, and the value is averaged by measurement in duplicate represented by the 2 curves (blue, red) on the graph. **B**, TAX2 or the scrambled peptide (100, 400, and 800 µmol/L) were incubated 3 min with human platelet-rich plasma (PRP) before addition of 1 or 0.75 µg/mL collagen, and platelet aggregation was monitored for 3 min by measuring light transmission using a Soderel Aggregometer. **C**, A representative curve for platelet aggregation in PRP induced by 1 µg/mL collagen is shown. **D**, Effect of TAX2 (800 µmol/L) on the lag phase after PRP activation by 1 or 0.75 µg/mL collagen. **E**, TAX2 or the scrambled peptide (100, 400, and 800 µmol/L) were incubated 3 min human washed platelets (WP) before addition of 4, 2, or 1 µg/mL collagen, and platelet aggregation was monitored for 3 min by measuring light transmission using a Soderel Aggregometer. **F**, A representative curve for platelet aggregation in WP induced by 4 µg/mL collagen is shown. **G**, Effect of TAX2 (800 µmol/L) on the lag phase after WP activation by 4, 2, or 1 µg/mL collagen. Data represent the mean±SEM of up to 3 (**A**, each performed at least in triplicate), 14 (**B** and **D**), and 10 (**E** and **G**) independent experiments (Student *t* test; **P*<0.05; ***P*<0.01; and ****P*<0.001, ns: nonsignificant). White bars, NaCl; grey bars, scrambled peptide; black bars, TAX2.

round of data indicates that TAX2 peptide significantly decreases human platelet aggregation.

Collagen-Induced Platelet Signaling Is Reduced by TAX2

To determine whether TAX2 inhibitory effect on platelet aggregation is also associated with decreased platelet signaling, washed platelets were stimulated by collagen, as an example of agonist, and then aggregation was stopped for further analysis of the platelet protein tyrosine phosphorylation profile. Of note, preincubation of resting platelets in presence of TAX2 up to 1 hour had no effect on protein tyrosine phosphorylation (data not shown). After 6 minutes aggregation, several platelet proteins were found to be phosphorylated on their tyrosine residues for both the control (NaCl) and scrambled peptide conditions, while preincubation in presence of TAX2 significantly decreased the tyrosine phosphorylation level of several signaling proteins (Figure 2A). To further confirm that TAX2 modulates the global platelet phosphoproteome in response to collagen stimulation, tyrosine-phosphorylated platelet proteins were immunoprecipitated using the 4G10 antibody, and a label-free quantitative proteomic analysis was conducted. The top 30 proteins identified in nonactivated platelets and collagen-activated platelets in presence of the scrambled

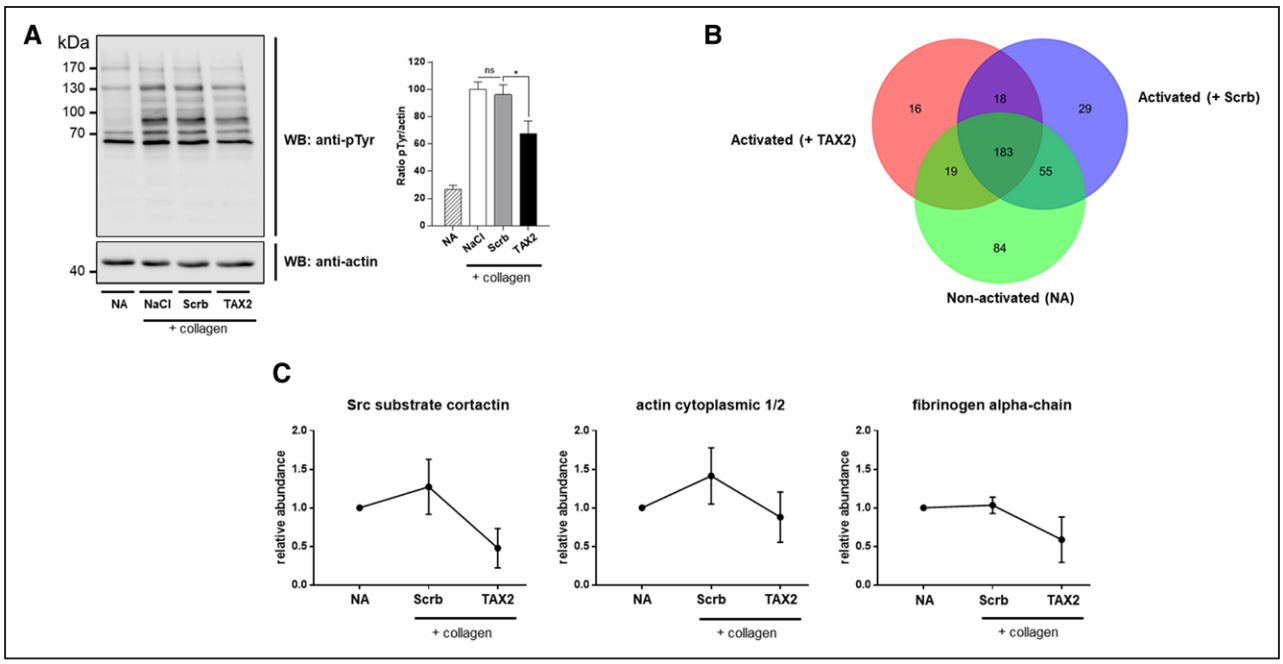

Figure 2. TAX2 peptide modulates collagen-induced platelet protein tyrosine phosphorylation.
A, Washed platelets were incubated with TAX2 or the scrambled peptide for 3 min before the addition of 4 µg/mL collagen, under stirring condition. After 6 min, platelet aggregates were solubilized by lysis buffer, and proteins separated by SDS-PAGE. **Left**, tyrosine-phosphorylated proteins were detected using the monoclonal 4G10 antibody and then protein amounts loaded were evaluated by an antiactin antibody. A representative tyrosine phosphorylation pattern of 3 independent experiments is shown. Quantification of tyrosine phosphorylation level was performed by densitometry analysis on all proteins exhibiting a molecular weight of at least 70 kDa. Results are expressed as mean±SEM of 3 independent experiments and normalized to the NaCl condition. (Student *t* test; **P*<0.05; ns: nonsignificant). **B**, Human washed platelets were incubated with TAX2 or the scrambled peptide for 3 min before addition of 4 µg/mL collagen, under stirring condition. After 3 min, aggregations were stopped by addition of lysis buffer, and equal amounts of proteins were subjected to immunoprecipitation using the 4G10 antibody. Proteins retained after 4G10 immunoprecipitation were digested with trypsin, analyzed by nano-LC-ESI MS/MS, and identified with PEAKS Studio software using the Swiss-Prot database. The Venn diagram represents the proteins identified in nonactivated platelets and collagen-activated platelets in presence of the scrambled peptide or TAX2 from 3 different donors. **C**, The number of spectra were used as a semiquantitative measure of the relative abundance of Src substrate cortactin, actin cytoplasmic 1/2 and fibrinogen α-chain. Results are expressed as mean±SEM of 3 independent experiments and normalized to the control condition. NA indicates nonactivated; and WB, Western blot.

peptide or TAX2 are shown in Tables I through IX in the Data Supplement. A total of 341, 285, and 236 proteins were unambiguously identified in nonactivated platelets and activated platelets in presence of the scrambled peptide or TAX2, respectively (Figure 2B). Among these proteins, 183 proteins were found in common, and 84, 29, and 16 proteins were identified exclusively in nonactivated platelets, activated platelets in presence of the scrambled peptide, or TAX2, respectively. As shown in Figure 2C, the relative abundance of key platelet proteins appears to be modulated under TAX2 treatment, as illustrated with Src substrate cortactin, actin, cytoplasmic 1/2, and fibrinogen α-chain. Taken together, these results strongly suggest that TAX2 inhibits platelet aggregation by modulating platelet signaling.

Platelet TSP-1:CD47 Interaction Is Disrupted by TAX2

To provide molecular insights and further ensure TAX2 specificity towards the TSP-1:CD47 axis, human and murine washed platelets were incubated with TAX2 or the scrambled peptide, and then reciprocal co-immunoprecipitations were performed using either anti-TSP-1 or anti-CD47 antibodies (Figure 3). Before that, platelets were stimulated with thrombin (0.2 IU/mL) for 5 minutes at room temperature without stirring to allow platelet activation without aggregation. When compared with the scrambled peptide, immunoprecipitation of CD47 from human (Figure 3A) and murine (Figure 3B) platelets led to a substantial decrease in the amount of co-immunoprecipitated TSP-1 in presence of TAX2 by 84.8±13.1% and 56.6±17.1%, respectively. Conversely, immunoprecipitation of TSP-1 from human platelets (Figure 3C) led to a consistent decrease by 65.3±19.5% in the amount of co-immunoprecipitated CD47 in presence of TAX2. When considering murine platelets (Figure 3D), co-immunoprecipitation of CD47 with TSP-1 was strongly decreased by 52.7±15.8%. While no significant interaction could be observed between TSP-1 and CD36 nor GPIb under our experimental conditions, TAX2 treatment did not alter the binding of TSP-1 to GPIIb-IIIa (Figure II in the Data Supplement). Taken together, these observations strongly suggest that TAX2 inhibits platelet

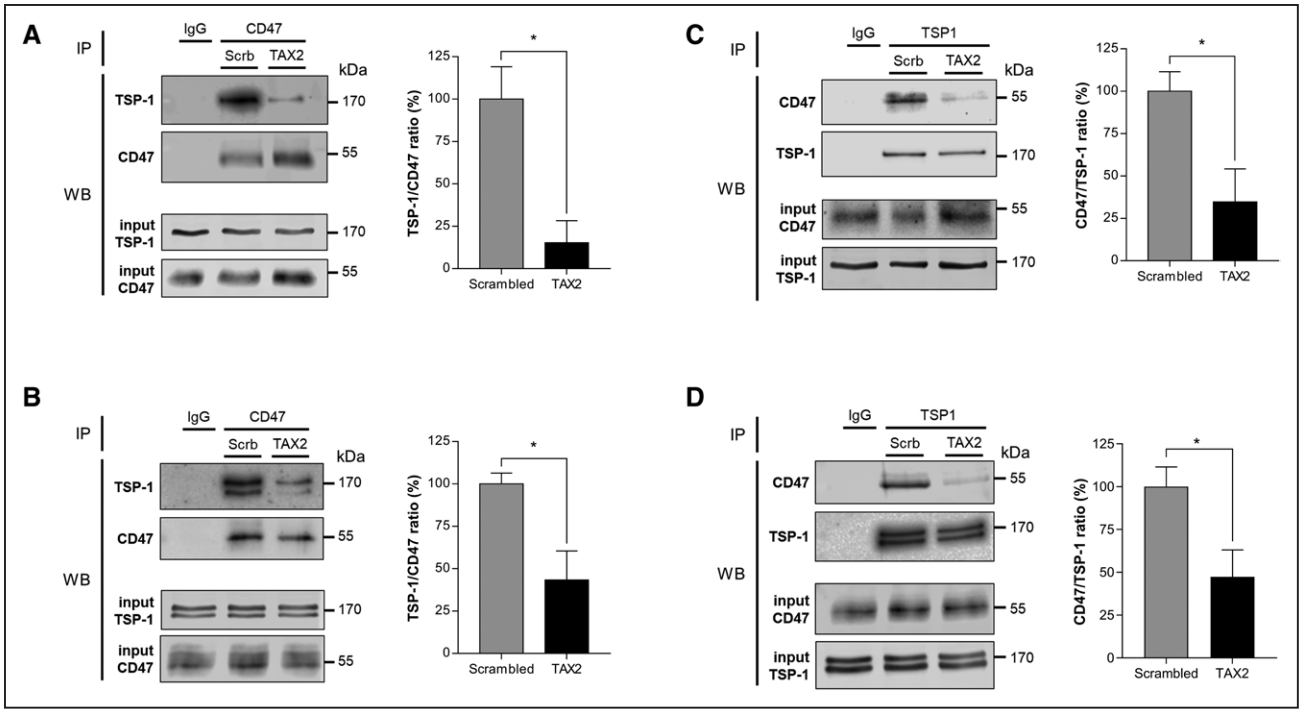

Figure 3. TAX2 peptide disrupts TSP-1 (thrombospondin-1):CD47 interaction in platelets.
CD47 was immunoprecipitated from human (**A**) or murine (**B**) washed platelets preincubated with thrombin (0.2 IU/mL) for 5 min at room temperature, without stirring, and with TAX2 or the scrambled peptide (800 µmol/L), and co-immunoprecipitation of TSP-1 was monitored by Western blot analysis. The **left** shows representative blots. **Right** graphs show blot quantification as determined by densitometry analysis. Results are expressed as mean±SEM of 4 (**A**) and 3 (**B**) independent experiments and normalized to the control condition (scrambled peptide). Student *t* test; **P*<0.05). **C** and **D**, TSP-1 was immunoprecipitated from human (**C**) or murine (**D**) washed platelets preincubated with thrombin (0.2 IU/mL) for 5 min at room temperature, without stirring, and with TAX2 or the scrambled peptide (800 µmol/L), and then co-immunoprecipitation of CD47 was monitored by Western blot analysis. The **left** shows representative blots. **Right** graphs show blot quantification as determined by densitometry analysis. Results are expressed as mean±SEM of 3 (**C**) or 4 (**D**) independent experiments and normalized to the control condition (scrambled peptide). ns indicates nonsignificant. Student *t* test; **P*<0.05. WB indicates Western blot.

aggregation and related signaling by specifically disrupting TSP-1:CD47 interaction.

Thrombus Formation In Vitro Is Delayed by TAX2

The effects of TAX2 on platelet function was further investigated by evaluating thrombus formation in vitro in the presence of TAX2 versus vehicle (NaCl 0.9%) in WT mice. To that purpose, whole blood perfusion assays were performed over a fibrillar collagen matrix at an arterial shear rate of 1500 s^{-1} (Figure 4). Platelet interaction with collagen under flow conditions requires the initial rolling and slowing down of platelets mainly through VWF immobilized onto collagen, before platelets adhere firmly to form thrombi. From 30 seconds, few adherent mouse platelets were observed, while after 5 minutes of perfusion the area covered by platelets was 56.5±4.5% in the vehicle group. In the presence of TAX2, thrombus formation was significantly delayed, and the area covered by platelets for WT mice was only 37.9±6.7% at 5 minutes (Figure 4A). Interestingly, perfusion of whole blood from *Thbs1*$^{-/-}$ mice, knock-out for the gene encoding TSP-1 (Figure III in the Data Supplement), led to an area covered by platelets (32.8±3.9%) similar to that of WT mice incubated with TAX2, at the end of perfusion. Whatever the time point being considered, preincubation with TAX2 had no further effect for *Thbs1*$^{-/-}$ mice. Moreover, compared with WT mice incubated with the vehicle, a significant decrease in the area covered by platelets was observed from 2 minutes for *Thbs1*$^{-/-}$ mice whereas the significance was only achieved at 3.5 minutes for the WT mice under TAX2 treatment (Figure 4A). Such observations do not rely on differences between *Thbs1*$^{-/-}$ and WT mice in surface expression levels of the main platelet receptors involved in such a process since comparable GPVI, GPIb, α_2, and GPIIb expression levels were observed between both genotypes, as evidenced using flow cytometry experiments (Figure IV in the Data Supplement). Similar experiments were performed with human whole blood. Before this, TAX2 stability was evaluated in freshly collected human plasma while incubating 1 µmol/L TAX2 during 2 hours at 37 °C. As shown in Figure V in the Data Supplement, TAX2 remained in the plasma after 2 hours' incubation without any observable degradation. Using human whole blood, and after 5 minutes of perfusion at 1500 s^{-1}, the area covered by platelets was 17.1±1.9% in the vehicle group and 16.7±2.0% for the scrambled peptide-treated group. In the presence of TAX2, the area covered by platelets was significantly decreased to

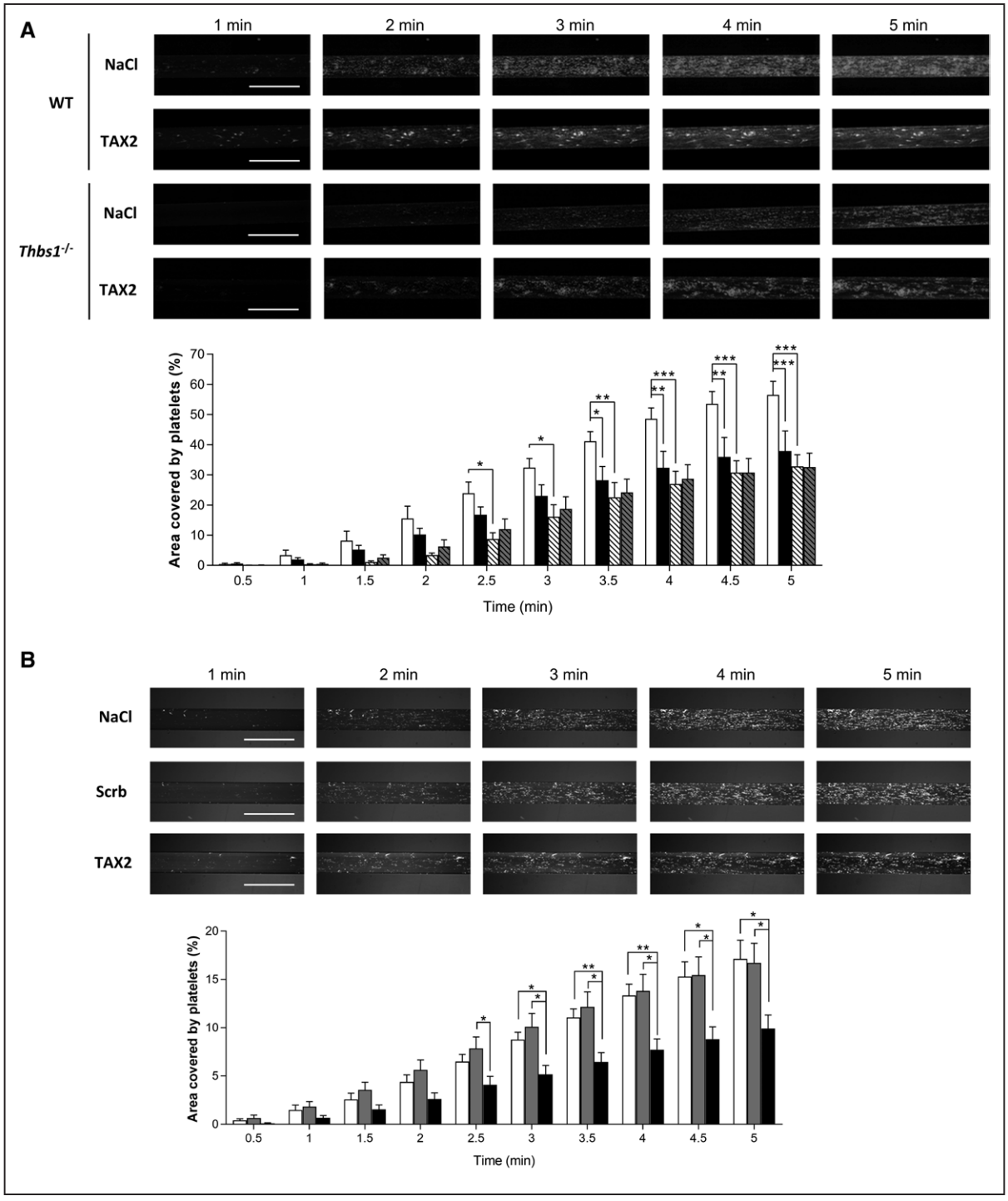

Figure 4. TAX2 peptide decreases platelet interaction onto collagen under arterial shear conditions.
A, Anticoagulated whole blood from wild-type (WT) or *Thbs1*$^{-/-}$ mice was incubated with rhodamine 6G (10 µg/mL) and either TAX2 peptide (100 µmol/L) or vehicle (NaCl 0.9%) for 10 min at 37°C before perfusion over a collagen matrix at 1500 s^{-1}. The progression of platelet adhesion and thrombi formation was observed under an epifluorescent microscope (overall magnification ×40). As an illustration, representative photographs at 1, 2, 3, 4, and 5 min are shown (**upper**, scale bars represent 1 mm). Results were expressed as the mean percentage of area covered by platelets±SEM of 6 (*Thbs1*$^{-/-}$) and 10 (wild-type) independent experiments (**down**). White bars, wild-type mice+NaCl 0.9%; black bars, wild-type mice+TAX2; white hatched bars, *Thbs1*$^{-/-}$ mice+NaCl 0.9%, gray hatched bars; *Thbs1*$^{-/-}$ mice+TAX2. (Two-way ANOVA with post hoc Tukey test; *P<0.05; **P<0.01; ***P<0.001; ns: nonsignificant). **B**, Anticoagulated human whole blood was incubated with rhodamine 6G (10 µg/mL) and either TAX2 peptide (100 µmol/L), scrambled peptide (100 µmol/L), or vehicle (NaCl 0.9%) for 10 min at 37°C before perfusion over a collagen matrix at 1500 s^{-1}. The progression of platelet adhesion and thrombi formation was observed under an epifluorescent microscope (overall magnification ×40). As an illustration, representative photographs for the three conditions (NaCl 0.9%, scrambled peptide, TAX2) at 1, 2, 3, 4, and 5 min are shown (**upper**, scale bars represent 1 mm). Results were expressed as the mean percentage of area covered by platelets±SEM of 11 (NaCl 0.9%, scrambled peptide) to 12 (TAX2) independent experiments (**down**). White bars, NaCl 0.9%; gray bars, scrambled peptide; black bars, TAX2. Two-way ANOVA with post hoc Tukey test. ns indicates nonsignificant. *P<0.05; **P<0.01; and ***P<0.001.

9.9±1.4% (Figure 4B). Together, these data strongly suggest that TSP-1:CD47 axis is important for thrombus formation in vitro under arterial shear conditions.

Thrombus Formation In Vivo, but not Bleeding Time, Is Delayed by TAX2

These in vitro results led us to investigate the effects of TAX2 in vivo using the $FeCl_3$-induced mesenteric arteriole and carotid artery thrombosis models. Ten minutes before the induction of thrombosis by 10% $FeCl_3$ for mesenteric arterioles (Figure 5A) or 7.5% $FeCl_3$ for carotid arteries (Figure 5B), mice were intravenously injected with either TAX2 peptide or the scrambled peptide at a 10 mg/kg BW dose, while vehicle (NaCl 0.9%)-treated group was used as reference. Treatment schedule was set in accordance with pharmacokinetics studies conducted in rats demonstrating TAX2 plasma half-life to vary between 15 minutes and 1 hour while being dose-dependent (data not shown). Time to complete thrombotic occlusion was monitored using real-time videomicroscopy and defined as an observed arrest in blood flow during at least 30 seconds. For WT mice, observed occlusion times were similar between vehicle (NaCl 0.9%) and scrambled peptide-treated groups. Occlusion times in the presence of vehicle were 26.1±3.7 and 11.4±0.7 minutes for mesenteric arterioles (Figure 5A) and carotid arteries (Figure 5B), respectively, while being measured at 21.7±4.4 (Figure 5A) and 10.5±1.2 (Figure 5B) minutes, respectively, in the presence of the scrambled peptide. Injection of TAX2 in these mice delayed by 2.4-fold (51.3±7.8 minutes, Figure 5A) and 1.7-fold (18.3±1.7 minutes, Figure 5B) occlusion times for mesenteric arterioles and carotid

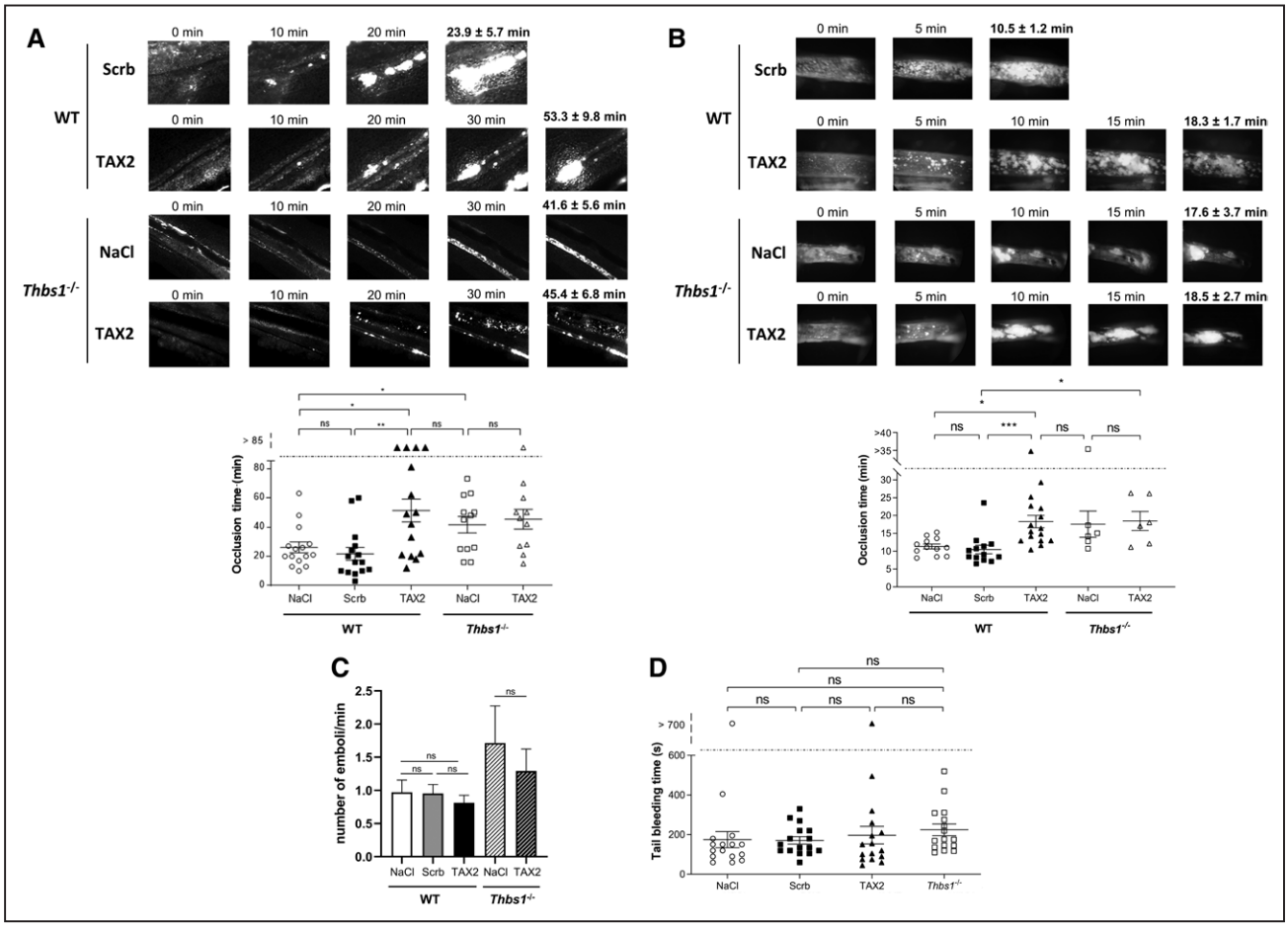

Figure 5. TAX2 treatment delays thrombus formation in vivo without affecting tail bleeding time.
Wild-type (WT) or *Thbs1*$^{-/-}$ mice were intravenously injected with TAX2 (10 mg/kg), the scrambled peptide (10 mg/kg), or vehicle (NaCl 0.9%) 10 min before the induction of thrombus formation by 10% $FeCl_3$ for mesenteric arterioles (**A**) or 7.5% $FeCl_3$ for carotid arteries (**B**). **Left** photographs show, as an illustration, a representative progression of thrombus formation for the different groups of mice. **Right** dot plots show times to complete thrombotic occlusion. The results are expressed as mean±SEM. ns indicates not significant (Mann-Whitney *U* test; **P*<0.05; ***P*<0.01; and ****P*<0.001). **C**, The number of emboli formed per minute during thrombus formation in carotid arteries of wild-type or *Thbs1*$^{-/-}$ mice intravenously injected with TAX2 (10 mg/kg), the scrambled peptide (10 mg/kg), or vehicle (NaCl 0.9%) was evaluated. Results are expressed as mean±SEM. (Mann-Whitney *U* test; ns: not significant). **D**, Tail bleeding times were measured on *Thbs1*$^{-/-}$ or wild-type mice intravenously injected with TAX2 (10 mg/kg), scrambled peptide (10 mg/kg), or vehicle (NaCl 0.9%) 5 min before tail cutting of. The results are expressed as mean±SEM. (Mann-Whitney *U* test; ns indicates not significant).

arteries, respectively. Importantly, *Thbs1*$^{-/-}$ mice showed prolonged occlusion times in the presence of vehicle, that were comparable to those observed from TAX2-treated WT mice in both mesenteric arteriole and carotid artery thrombosis models (Figure 5A and 5B). Consistently, no significant change was measured in *Thbs1*$^{-/-}$ mice under TAX2 treatment. Overall, these observations demonstrate that TAX2 exhibits robust antithrombotic properties in these 2 murine models of thrombosis. We also evaluated the impact of TAX2 treatment on the number of emboli released per minute during thrombus formation in carotid arteries of mice, and no significant differences were observed between the different groups. The mean number of emboli per minute was 1.0±0.2, 1.0±0.1, and 0.8±0.1 for NaCl-, scrambled peptide- and TAX2-treated WT mice, respectively (Figure 5C). For *Thbs1*$^{-/-}$ mice, the number of emboli released per minute reached 1.7±0.6 for NaCl- and 1.3±0.3 for TAX2-treated mice (Figure 5C). Antiplatelet therapy is associated with increased rates of bleeding,[1,2] hence development of new strategies for management of severe bleeding in the setting of antiplatelet therapy is of primary importance. To determine whether TAX2 therapy may affect bleeding tendency, tail bleeding times were measured in WT mice injected with vehicle, scrambled peptide (10 mg/kg), or TAX2 (10 mg/kg) and then compared with those observed from *Thbs1*$^{-/-}$ mice. As shown in Figure 5E, tail bleeding times in mice injected with TAX2 were remarkably comparable to vehicle- and scrambled peptide-treated groups, as well as to *Thbs1*$^{-/-}$ mice. We finally compared bleeding times of TAX2-administrated mice with mice receiving an antiplatelet drug widely used in clinics, the P2Y12 antagonist clopidogrel,[30] at a concentration that has comparable effect to the antithrombotic effect of TAX2. When administrated intravenously at 5 mg/kg, clopidogrel led to a delay in carotid occlusion times (20.6±2.2 minutes) comparable to TAX2-treated mice (18.3±1.7 minutes, Figure VI in the Data Supplement). At this concentration of clopidogrel, physiological hemostasis was drastically impacted since no cessation of bleeding was observed for all treated mice at 15 minutes (Figure VI in the Data Supplement). Together, these data strengthen the safety profile of TAX2 and its advantages regarding bleeding tendency.

Characterization of TAX2 Peptide Safety Profile

The above-detailed results shed light on promising antithrombotic properties for TAX2 peptide being associated with low risk of bleeding. This led us to evaluate acute and repeated dosing toxicity of TAX2 to ensure innocuity. As illustrated in Figure VII in the Data Supplement, sequence alignments showed that TAX2 target sequence on TSP-1 C-terminal domain (^{1034}RFYVVMWK^{1041}) is conserved between mice and rats, as well as in all the vertebrates evaluated. TAX2 was intraperitoneally administered in rats at 100, 300, and 400 mg/kg doses either considering a single bolus administration (acute toxicity) or QDx7 (repeated toxicity), and then different parameters were evaluated. As shown in Figure 6, all rats administered with QDx7 TAX2 peptide appeared healthy during the study, and no notable body weight or food consumption changes were observed (Figure 6A through 6C). Compared with vehicle-treated animals, no effect was observed on organ (heart, lungs, liver, kidneys, pancreas, spleen, intestines, ovaries, and testes) weights in both genders (Figure 6D and 6E). Hemoglobin, red blood cells count, and hematocrit in TAX2-treated groups remained nearly unchanged compared with the vehicle-treated rats (Figure 6F through 6K). Potential toxicity of TAX2 regarding platelet counts, prothrombin time, and activated partial thromboplastin times was also evaluated from freshly collected blood samples. For both procedures (acute and repeated toxicity), increasing administrations of TAX2 up to 400 mg/kg had no major incidence on both the coagulation parameters and platelet counts (Table) although statistically significant differences were observed between TAX2- and vehicle-treated groups for some values. However, platelet counts were within the normal range already described for Sprague Dawley rats,[31] and no dose-response relationship was observed for prothrombin time and activated partial thromboplastin time values, further suggesting that these small but significant differences were rather incidental. Absence of noticeable toxicity of TAX2 was also observed in mice (data not shown). Considering a 30 mg/kg dose of TAX2 peptide, that is, 3× higher than reported antithrombotic efficacy dose, no deleterious effects were observed regarding platelet counts and mean platelet volume. Taken together, these data stressed the safety profile of TAX2 in these preclinical conditions. Finally, we also assessed plasma VWF antigen and multimeric structure under acute or repeated administration of 100 mg/kg TAX2 in mice. As shown in Figure VIII in the Data Supplement, plasma VWF antigen levels were similar between vehicle- and TAX2-treated groups for both procedures and a partial loss of the HMW (high-molecular-weight) multimers of VWF, that remains to be further confirmed, was observed in 60% of the mice under chronic administration of TAX2. Together, these results highlight the safety of TAX2 peptide in rodents.

DISCUSSION

Studies from human and murine platelets have shown that TSP-1 is involved in platelet activation and aggregation[18,32,33] and in stabilization of platelet aggregates by forming bridges between fibrinogen molecules bound to platelet GPIIb/IIIa.[8] Even if TSP-1 function may be considered as redundant for platelet aggregation, TSP-1 is also known to indirectly influence platelet activity via binding to several matrix proteins such as collagen,

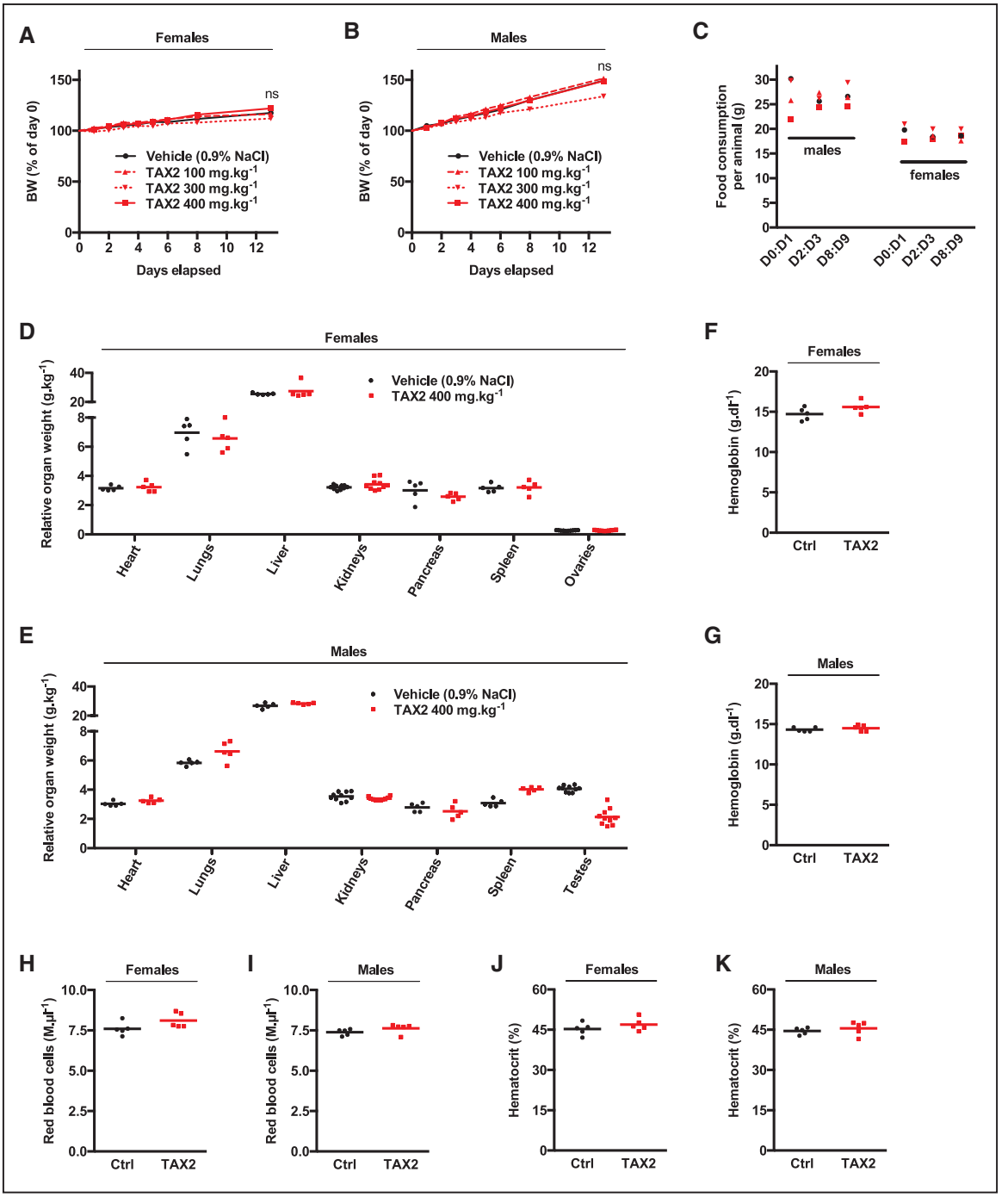

Figure 6. Evaluation of TAX2 peptide toxicity in rats.

A–**K**, The potential toxicity of TAX2 peptide being intraperitoneally administered to Sprague Dawley rats (5 male and 5 female rats per group) once daily for 7 consecutive days at doses of 100, 300, and 400 mg·kg^{-1} was assessed (dosing from day 1–7, follow-up to day 14), while reference control group (*Ctrl*) received the vehicle alone (0.9% NaCl). **A** and **B**, Evolution of rat (females **A** and males **B**) body weights, expressed as a percentage of day 0 (mean±SEM, n=5 per group). For each group, values were compared with control group using 1-way ANOVA followed by Dunnett post hoc test (ns indicates not significant). **C**, Food consumption measurements in male and female groups (0.9 % NaCl, ▲ TAX2 100 mg·kg^{-1}, ▼ TAX2 300 mg·kg^{-1}, ■ TAX2 400 mg·kg^{-1}). Food consumption for a 24 h period was performed once during study initiation (days 0:1) and thereafter once a week (days 2:3 and 8:9). Determinations of food consumption (calculated value) were based on a provided diet per groups of 3 or 2 animals per cage. **D** and **E**, At day 14 (necropsy) and after postmortem examination, the following selected organs from control and high dose (TAX2 300 mg·kg^{-1}) groups were collected and then wet weighed: heart, kidneys, liver, lungs, pancreas, spleen, ovaries/testes. For lungs weighing, heart, and lungs were weighed together, and then heart weight was subtracted. Scatter dot plots report weighing measurements expressed as relative organ to body weights ratios (n=5 per group; line, mean). **F**–**K**, Blood hematology results for control and high dose groups. On day 14, blood samples (≈300–500 µL) were collected into EDTA tubes and then hematology analysis was performed including hemoglobin dosing (**F**–**G**), red blood cells count (**H**–**I**), and hematocrit determination (**J**–**K**) as reported in the scatter dot plots (line, mean).

Table. Evaluation of TAX2 Peptide Toxicity on the Platelet Count and Coagulation Parameters in Rats

	Platelet count, ×103/µL		PT, s		aPTT, s	
Female	D2	D15	D2	D15	D2	D15
NaCl 0.9%	404.0±29.2	644.5±113.0	30.3±3.8	29.3±1.3	88.0±14.0	72.8±3.2
TAX2 100 mg/kg	550.0±11.0	733.4±70.1	25.7±0.9	32.8±4.8	69.0±6.4	89.5±12.9
TAX2 300 mg/kg	743.5±66.9*	798.0±87.3	27.2±0.5	26.3±1.5	65.0±4.1*	68.0±3.9
TAX2 400 mg/kg	731.0±112.9*	863.4±98.8	26.3±0.5	26.7±0.9	83.3±1.3	67.3±2.8
Male	D2	D15	D2	D15	D2	D15
NaCl 0.9%	512.3±47.7	662.6±147.2	26.8±0.9	30.0±0.4	59.0±1.3	67.2±4.1
TAX2 100 mg/kg	635.8±63.4	523.4±127.3	28.4±1.4	29.2±1.8	72.8±8.8	70.0±6.2
TAX2 300 mg/kg	665.0±150.4	813.8±50.8	24.2±1.2	24.4±0.9	65.8±1.9	59.8±1.0
TAX2 400 mg/kg	718.0±102.7	757.6±72.5	27.0±1.1	30.8±2.9	70.2±4.6	64.3±0.9
Female	D-1	D15	D-1	D15	D-1	D15
NaCl 0.9%	540.7±175.8	695.4±109.7	26.7±1.8	27.3±0.9	68.7±4.8	69.0±1.3
TAX2 100 mg/kg	471.5±101.3	856.2±43.9	27.3±0.9	22.8±0.9	71.0±5.7	86.2±4.6*
TAX2 300 mg/kg	681.4±67.8	777.5±106.4	23.0±0.0	27.4±2.5	66.0±2.1	65.6±5.7
TAX2 400 mg/kg	784.8±38.6	902.6±24.2	24.6±1.3	26.0±1.6	77.2±4.5	64.0±3.9
Male	D-1	D15	D-1	D15	D-1	D15
NaCl 0.9%	495.6±73.7	937.6±39.8	26.8±0.2	26.6±0.7	67.8±3.8	72.4±2.7
TAX2 100 mg/kg	634.0±96.0	760.8±71.3	26.4±1.2	24.2±1.1	72.3±3.3	63.2±1.2
TAX2 300 mg/kg	914.8±32.3†	703.5±142.6	23.8±0.7*	25.0±0.9	68.4±3.3	64.0±5.7
TAX2 400 mg/kg	622.3±131.5	725.2±109.2	27.0±1.0	23.2±1.2	66.0±17.0	65.3±4.0

Male and female Sprague Dawley rats (5 males and 5 females per group) were intraperitoneally injected with a single dose of TAX2 (100, 300, and 400 mg/kg) or vehicle (NaCl 0.9%) for evaluation of acute toxicity on platelet count and coagulation parameters on day 2 (D2) and day 15 (D15) after injection. Male and female Sprague Dawley rats (5 males and 5 females per group) were daily and for 7 consecutive days intraperitoneally injected with TAX2 (100, 300, and 400 mg/kg) or vehicle (NaCl 0.9%) for evaluation of repeated dosing toxicity considering platelet count and coagulation parameters on day 15 (D15). Platelet count and coagulation parameters were also measured 1 day before the first injection (D-1). The results are expressed as mean±SEM; 1-way ANOVA. aPTT indicates activated partial thromboplastin time; and PT, prothrombin time.

*$P<0.05$.

†$P<0.01$ vs NaCl 0.9%.

hence modulating platelet phosphatidylserine exposure and thrombus stability,[34] or to von Willebrand factor by protecting the latter from cleavage by matrix proteinases.[13] Recent data also suggest that the release of TSP-1 regulates hemostasis in vivo through modulation of platelet cAMP signaling at sites of vascular injury.[35] Together, these data argue in favor of an important role of TSP-1 in thrombogenic conditions.

In this study, we hypothesized that platelet TSP-1:CD47 axis may be a promising target for antithrombotic therapy. The recently engineered TAX2 peptide[19] was considered together with *Thbs1*$^{-/-}$ mice so as to provide strong evidence validating the therapeutic relevance of specifically inhibiting CD47 activation by TSP-1. Peptides have gained increased interest as therapeutics during recent years. Therapeutic peptides offer several advantages over proteins or antibodies as they have high activity, specificity, and affinity. They are also small-sized, easy to synthesize, and putatively less immunogenic than recombinant proteins or antibodies.[36] TAX2 is a CD47-derived peptide that directly binds the cell-binding domain of TSP-1[20] and specifically antagonizes TSP-1:CD47 interaction as evidenced here by reciprocal co-immunoprecipitation experiments from thrombin-activated human and mouse washed platelets. No interference was observed on TSP-1 interaction with GPIIb/IIIa. Since we failed to demonstrate an interaction between TSP-1 and CD36 or GPIb in our conditions, potential interference of TAX2 on the interaction of TSP-1 with both platelet receptors cannot be excluded. Multiple sequence alignments also show that TSP-1 sequence (RFYVVMWK) targeted by TAX2 is highly conserved between species.

In the present study, blocking TSP-1:CD47 axis using TAX2 antagonization was shown to dose-dependently and drastically inhibit human platelet aggregation induced by different agonists in whole blood and PRP, when compared with a control peptide. The strongest inhibitory effect of TAX2 was observed on washed platelets with a decrease of about 75% and 85% for collagen- and TRAP-6-induced washed platelet aggregation, respectively, when low doses of agonists were used. Discrepancies observed between washed platelets and platelets in whole blood or in PRP may be due to the fraction of TAX2 peptide being bound to plasma proteins (data not shown). Of note, a trend for increase of the lag phase during collagen-induced platelet aggregation in whole blood, PRP and washed platelets, was observed under TAX2 application. Although GPVI is the main activator

receptor being involved in platelet aggregation induced by fibrillar collagen,[37,38] the previously reported synergistic effect of TSP-1:CD47 axis on $\alpha_2\beta_1$-mediated platelet signaling and activation induced by collagen[16] may also account in the prolongation of the lag phase observed in presence of TAX2. Further studies have also demonstrated that the potentiating effect of TSP-1 on platelet activation and aggregation involves binding of TSP-1 to CD47 and inhibition of the antithrombotic activity of the NO/cGMP pathway.[18] This inhibitory effect of TSP-1 on soluble guanylate cyclase seems to be a universal regulatory mechanism that may have important implications in cardiovascular function.[39,40]

The inhibitory action of TAX2 also involves modulation of platelet signaling as evidenced here by the significant reduction of the phosphorylation pattern observed for TAX2-treated platelets in response to collagen activation. These results are strengthened by our proteomics data. Although additional experiments are required, they show that TAX2 may modulate the global phosphoproteome of platelets in response to agonist stimulation. Together, these results support the potentiating role of the TSP-1:CD47 axis in platelet activation and aggregation[15,16,32,41,42] while demonstrating that TAX2 peptide exhibits platelet antiaggregant properties.

In this study, we also highlight that antagonizing TSP-1:CD47 axis using TAX2 therapy strongly reduces human and mouse platelet interaction and subsequent thrombus formation onto immobilized collagen under arterial shear conditions. Platelet interaction with collagen under flow conditions requires the initial tethering of platelets mediated by VWF binding to platelet GPIb to allow engagement of adhesive platelet receptors into firm adhesion and subsequent thrombus formation.[43] Although a slight decrease was observed from the early minutes of perfusion under TAX2 treatment, the area covered by mouse and human platelets was strongly decreased by about 33% and 42%, respectively, in the presence of TAX2 when compared with the control condition. The same experiments were performed concomitantly considering blood samples obtained from *Thbs1*$^{-/-}$ mice. In these conditions, a decrease in the area covered by platelets was observed from the early phases of perfusion, being putatively due to the protective role of TSP-1 towards proteolytic degradation of VWF. The platelet-tethering function of VWF is indeed proteolytically regulated by ADAMTS13 and previous works have demonstrated that soluble or local platelet-released TSP-1 has a protective role towards VWF while preventing its degradation by this plasma protease.[13,44] Of note, *Thbs1*$^{-/-}$ mice have platelet surface expression levels of GPVI, GPIb, α_2, and GPIIb being comparable to WT mice. After 5 minutes of perfusion, the area covered by platelets being devoid of TSP-1 was, however, decreased to a similar extent to what observed from WT mice in the presence of TAX2. Together, these data demonstrate that blocking TSP-1:CD47 interaction by TAX2 exhibits strong inhibition of thrombus formation onto immobilized collagen under arterial shear conditions. Moreover, the fact that TAX2 mimics the effects of *Thbs1*$^{-/-}$ mice argues in favor of a critical role for the TSP-1:CD47 axis in such a process. This led us to investigate the effects of TAX2 treatment using in vivo models of arterial thrombosis.

We considered the $FeCl_3$-induced thrombosis model which is one of the most widely used murine models and a valuable tool for therapy evaluation in the treatment and prevention of thrombotic and atherothrombotic diseases.[45–47] In contrast to vehicle and the scrambled peptide, we found that a single 10 mg/kg intravenous administration of TAX2 peptide in WT mice led to a significant delay of the time to complete arterial occlusion both in the mesenteric arteriole and the carotid artery, as 2.4- and 1.7-fold increases were observed, respectively. Interestingly, times to complete vessel occlusion were prolonged to a similar extent in *Thbs1*$^{-/-}$ mice while administration of TAX2 peptide in these knock-out mice had no further effect. Here again, these results demonstrate that the sole antagonization of TSP-1:CD47 interaction by TAX2 is sufficient to reproduce the antithrombotic effects observed in *Thbs1*$^{-/-}$ mice, and further strengthen the critical role played by the TSP-1:CD47 axis in arterial thrombosis. When looking at the number of emboli released per minute during thrombus formation in carotid arteries, no difference was observed between the different groups, suggesting that TAX2 has no effect on thrombus stability and embolization.

Importantly, bleeding times measured from sectioned mice tails suggest that TAX2 treatment is not likely to be associated with increased bleeding tendency, as well as deficiency of TSP-1 in mice.[48] These observations are of great interest since current therapies using antiplatelet agents are associated with increased bleeding risk and are, therefore, subjected to contraindications.[2,3] This is exemplified by a recent study from comparable animal models of $FeCl_3$-induced thrombosis that reported that administration of clopidogrel by gavage (30 mg/kg per day, 2 days) delays thrombus formation within a similar range than TAX2 does, while increasing bleeding time by >2-fold in the tail bleeding assay.[49] Here, we showed that at a concentration of clopidogrel (5 mg/kg, IV injection) that delays thrombus formation within a similar range than TAX2 does, no cessation of bleeding was observed for all the tested mice at 15 minutes. Therefore, these data argue that for a given concentration leading to comparable antithrombotic properties, TAX2 shows benefits compared with current antiplatelet drugs regarding bleeding risk.

Moreover, results arising from toxicity studies conducted in rats highlighted that TAX2 has a safe profile up to the 400 mg/kg (ie, a therapeutic index of 40 when looking at efficiency being observed in chemically induced thrombosis models), and this regarding several

parameters such as weight, anemia, platelet count as well as coagulation parameters. In 60% of tested mice, a partial loss of the HMW multimers of VWF has been observed only under chronic administration of 100 mg/kg TAX2. In addition to ADAMTS13,[13] other proteases have been shown to cleave VWF such as neutrophil elastase, proteinase 3, cathepsin G, matrix metalloproteinase 9, or plasmin.[50,51] Whether this partial loss of the HMW multimers of VWF is due to a differential TSP-1 bioavailability protecting against degradation by ADAMTS13, or to activation of other proteases, remains to be determined. Another possible explanation may arise from TAX2 binding to TSP-1 that impedes TSP-1 interaction with the A2 and A3 domains of VWF.[52]

Finally, even if the multimodular nature of TSP-1 enables it to interact with many other platelet receptors, several integrins and other adhesive matrix glycoproteins, and despite the remaining controversy about their respective roles, this study strengthens the critical role played by the TSP-1:CD47 axis during platelet activation and thrombosis. In addition, these pioneering results demonstrate that TAX2 peptide should be considered as a new strategy of high therapeutic interest in controlling platelet activation and related thrombotic disorders, while being associated with an apparently favorable safety profile and low bleeding risk. Dual antiplatelet therapies have shown their incremental benefit and efficacy. However, bleeding remains a major limitation of current therapeutic approaches, and the adverse effects of bleeding on mortality and cardiovascular outcomes might offset the benefit of potent antiplatelet strategies.[53] Therefore, new antiplatelet agents are continually needed and antagonization of TSP-1-CD47 may be considered as one of these new options. To be a viable therapeutic, a meaningful half-life in circulation is required. From pharmacokinetic evaluations in rats (data not shown), TAX2 half-life in the circulation was shown to vary between 15 minutes and 1 hour and to be dose-dependent, that is quite common for therapeutic peptides. Additional developments are likely to extend TAX2 half-life in the circulation, such as parenteral formulation development, peptide conjugates, PEGylation or incorporation of non-natural amino acids. However, the fast uptake of TAX2 drug candidate reported here represents an advantage over current antiplatelet treatments, especially in the case of ischemic stroke or heart attack where emergency therapy needs to be delivered rapidly after the onset of symptoms.

Note

TAX2 peptide was filed for an international patent (WO/2013/007933 A1). The acute and repeated dosing toxicity studies of TAX2 were supervised by Pharmaseed Ltd. and performed at the 4P-Pharma test site (Lille, France).

ARTICLE INFORMATION

Received March 31, 2020; accepted November 11, 2020.

Affiliations

UMR CNRS 7369 Matrice Extracellulaire et Dynamique Cellulaire (MEDyC), Université de Reims Champagne Ardenne (URCA), UFR Sciences Exactes et Naturelles, Reims, France (A.J., T.S., M.C., C.K., L.M., P.M., S.D.). SATT Nord, Lille, France (A.J.). Apmonia Therapeutics, Reims, France (A.J., S.D.). HITh, UMR_S 1176, INSERM Univ. Paris-Sud, Université Paris-Saclay, France (A.K.). Fraunhofer Institute for Microstructure of Materials and Systems IMWS, Halle (Saale), Germany (T.H., C.E.H.S.).

Acknowledgments

We gratefully acknowledge Dr Revital Rattenbach, Dr Céline Martin, Dr Aurélie Docquier (4P-Pharma, Lille, France), and Dr Itschak Lamensdorf (Pharmaseed Ltd, Ness Ziona, Israel) for their contribution in designing and conducting the preclinical toxicity studies. We are also very grateful to Dr Damien Rioult, Dr Jérémy Ortillon, Olivier Bocquet, Cathy Hachet, and Christian Ihling for their technical assistance as well as the anonymous blood donors of the EFS Grand Est. Aggregometry assays were performed with the material support of the Hemostasis and Post-Ischemia Vascular Remodeling Unit (HERVI, EA3801) of Reims University Hospital Center (Pr Philippe Nguyen). We also thank Jean-Luc Breda, Anthony Pigeon, and Perrine Manot for animal care. A. Jeanne designed the project and performed experiments. T. Sarazin, M. Charlé, C. Kawecki, A. Kauskot, T. Hedtke, and C.E.H. Schmelzer performed experiments. P. Maurice and S. Dedieu conceived, designed, and supervised the study. A. Jeanne, T. Sarazin, P. Maurice, and S. Dedieu were involved in writing the article and preparing the figures. L. Martiny contributed to review the article.

Sources of Funding

This work was supported by grants from SATT Nord, CNRS, URCA, Région Grand Est, the Fondation de France and the Fraunhofer Attract program (grant 069-608203). Apmonia Therapeutics provided financial support for safety assessment of TAX2 peptide and efficacy studies in mice. A. Jeanne was supported by SATT Nord (2014-2019). T. Sarazin was PhD fellow supported by URCA and Région Grand-Est (2017-2020). C. Kawecki was PhD fellow supported by the Région Champagne-Ardenne.

Disclosures

A. Jeanne and S. Dedieu serve as President and Chair of the Scientific and Clinical Advisory Board, respectively, and have equity interest in Apmonia Therapeutics (Reims, France) that licensed TAX2 technology for translational development. The other authors report no conflicts.

REFERENCES

1. Benjamin EJ, Virani SS, Callaway CW, Chamberlain AM, Chang AR, Cheng S, Chiuve SE, Cushman M, Delling FN, Deo R, et al; American Heart Association Council on Epidemiology and Prevention Statistics Committee and Stroke Statistics Subcommittee. Heart disease and stroke statistics-2018 update: a report from the american heart association. *Circulation*. 2018;137:e67–e492. doi: 10.1161/CIR.0000000000000558
2. Melkonian M, Jarzebowski W, Pautas E, Siguret V, Belmin J, Lafuente-Lafuente C. Bleeding risk of antiplatelet drugs compared with oral anticoagulants in older patients with atrial fibrillation: a systematic review and meta-analysis. *J Thromb Haemost*. 2017;15:1500–1510. doi: 10.1111/jth.13697
3. Nathan AS, Sen S, Yeh RW. The risk of bleeding with the use of antiplatelet agents for the treatment of cardiovascular disease. *Expert Opin Drug Saf*. 2017;16:561–572. doi: 10.1080/14740338.2017.1315101
4. Koupenova M, Kehrel BE, Corkrey HA, Freedman JE. Thrombosis and platelets: an update. *Eur Heart J*. 2017;38:785–791. doi: 10.1093/eurheartj/ehw550
5. Dubernard V, Arbeille BB, Lemesle MB, Legrand C. Evidence for an alpha-granular pool of the cytoskeletal protein alpha-actinin in human platelets that redistributes with the adhesive glycoprotein thrombospondin-1 during the exocytotic process. *Arterioscler Thromb Vasc Biol*. 1997;17:2293–2305. doi: 10.1161/01.atv.17.10.2293
6. Novelli EM, Kato GJ, Ragni MV, Zhang Y, Hildesheim ME, Nouraie M, Barge S, Meyer MP, Hassett AC, Gordeuk VR, et al. Plasma thrombospondin-1 is increased during acute sickle cell vaso-occlusive events and associated with acute chest syndrome, hydroxyurea therapy, and lower hemolytic rates. *Am J Hematol*. 2012;87:326–330. doi: 10.1002/ajh.22274

7. Lawler J. The functions of thrombospondin-1 and-2. *Curr Opin Cell Biol.* 2000;12:634–640. doi: 10.1016/s0955-0674(00)00143-5
8. Bonnefoy A, Hantgan R, Legrand C, Frojmovic MM. A model of platelet aggregation involving multiple interactions of thrombospondin-1, fibrinogen, and GPIIbIIIa receptor. *J Biol Chem.* 2001;276:5605–5612. doi: 10.1074/jbc.M010091200
9. Jurk K, Clemetson KJ, de Groot PG, Brodde MF, Steiner M, Savion N, Varon D, Sixma JJ, Van Aken H, Kehrel BE. Thrombospondin-1 mediates platelet adhesion at high shear via glycoprotein Ib (GPIb): an alternative/backup mechanism to von Willebrand factor. *FASEB J.* 2003;17:1490–1492. doi: 10.1096/fj.02-0830fje
10. Frieda S, Pearce A, Wu J, Silverstein RL. Recombinant GST/CD36 fusion proteins define a thrombospondin binding domain. Evidence for a single calcium-dependent binding site on CD36. *J Biol Chem.* 1995;270:2981–2986. doi: 10.1074/jbc.270.7.2981
11. Gao AG, Lindberg FP, Finn MB, Blystone SD, Brown EJ, Frazier WA. Integrin-associated protein is a receptor for the C-terminal domain of thrombospondin. *J Biol Chem.* 1996;271:21–24. doi: 10.1074/jbc.271.1.21
12. Prakash P, Kulkarni PP, Chauhan AK. Thrombospondin 1 requires von Willebrand factor to modulate arterial thrombosis in mice. *Blood.* 2015;125:399–406. doi: 10.1182/blood-2014-06-581942
13. Bonnefoy A, Daenens K, Feys HB, De Vos R, Vandervoort P, Vermylen J, Lawler J, Hoylaerts MF. Thrombospondin-1 controls vascular platelet recruitment and thrombus adherence in mice by protecting (sub)endothelial VWF from cleavage by ADAMTS13. *Blood.* 2006;107:955–964. doi: 10.1182/blood-2004-12-4856
14. Lindberg FP, Gresham HD, Schwarz E, Brown EJ. Molecular cloning of integrin-associated protein: an immunoglobulin family member with multiple membrane-spanning domains implicated in alpha v beta 3-dependent ligand binding. *J Cell Biol.* 1993;123:485–496. doi: 10.1083/jcb.123.2.485
15. Chung J, Gao AG, Frazier WA. Thrombspondin acts via integrin-associated protein to activate the platelet integrin alphaIIbbeta3. *J Biol Chem.* 1997;272:14740–14746. doi: 10.1074/jbc.272.23.14740
16. Chung J, Wang XQ, Lindberg FP, Frazier WA. Thrombospondin-1 acts via IAP/CD47 to synergize with collagen in alpha2beta1-mediated platelet activation. *Blood.* 1999;94:642–648.
17. Lagadec P, Dejoux O, Ticchioni M, Cottrez F, Johansen M, Brown EJ, Bernard A. Involvement of a CD47-dependent pathway in platelet adhesion on inflamed vascular endothelium under flow. *Blood.* 2003;101:4836–4843. doi: 10.1182/blood-2002-11-3483
18. Isenberg JS, Romeo MJ, Yu C, Yu CK, Nghiem K, Monsale J, Rick ME, Wink DA, Frazier WA, Roberts DD. Thrombospondin-1 stimulates platelet aggregation by blocking the antithrombotic activity of nitric oxide/cGMP signaling. *Blood.* 2008;111:613–623. doi: 10.1182/blood-2007-06-098392
19. Jeanne A, Sick E, Devy J, Floquet N, Belloy N, Theret L, Boulagnon-Rombi C, Diebold MD, Dauchez M, Martiny L, et al. Identification of TAX2 peptide as a new unpredicted anti-cancer agent. *Oncotarget.* 2015;6:17981–18000. doi: 10.18632/oncotarget.4025
20. Jeanne A, Boulagnon-Rombi C, Devy J, Théret L, Fichel C, Bouland N, Diebold MD, Martiny L, Schneider C, Dedieu S. Matricellular TSP-1 as a target of interest for impeding melanoma spreading: towards a therapeutic use for TAX2 peptide. *Clin Exp Metastasis.* 2016;33:637–649. doi: 10.1007/s10585-016-9803-0
21. Jeanne A, Martiny L, Dedieu S. Thrombospondin-targeting TAX2 peptide impairs tumor growth in preclinical mouse models of childhood neuroblastoma. *Pediatr Res.* 2017;81:480–488. doi: 10.1038/pr.2016.242
22. Daubon T, Léon C, Clarke K, Andrique L, Salabert L, Darbo E, Pineau R, Guérit S, Maitre M, Dedieu S, et al. Deciphering the complex role of thrombospondin-1 in glioblastoma development. *Nat Commun.* 2019;10:1146. doi: 10.1038/s41467-019-08480-y
23. Jeanne A, Untereiner V, Perreau C, Proult I, Gobinet C, Boulagnon-Rombi C, Terryn C, Martiny L, Brézillon S, Dedieu S. Lumican delays melanoma growth in mice and drives tumor molecular assembly as well as response to matrix-targeted TAX2 therapeutic peptide. *Sci Rep.* 2017;7:7700. doi: 10.1038/s41598-017-07043-9
24. Turriziani B, Garcia-Munoz A, Pilkington R, Raso C, Kolch W, von Kriegsheim A. On-beads digestion in conjunction with data-dependent mass spectrometry: a shortcut to quantitative and dynamic interaction proteomics. *Biology (Basel).* 2014;3:320–332. doi: 10.3390/biology3020320
25. de Witt SM, Swieringa F, Cavill R, Lamers MM, van Kruchten R, Mastenbroek T, Baaten C, Coort S, Pugh N, Schulz A, et al. Identification of platelet function defects by multi-parameter assessment of thrombus formation. *Nat Commun.* 2014;5:4257. doi: 10.1038/ncomms5257
26. Kawecki C, Hézard N, Bocquet O, Poitevin G, Rabenoelina F, Kauskot A, Duca L, Blaise S, Romier B, Martiny L, et al. Elastin-derived peptides are new regulators of thrombosis. *Arterioscler Thromb Vasc Biol.* 2014;34:2570–2578. doi: 10.1161/ATVBAHA.114.304432
27. Li W, McIntyre TM, Silverstein RL. Ferric chloride-induced murine carotid arterial injury: a model of redox pathology. *Redox Biol.* 2013;1:50–55. doi: 10.1016/j.redox.2012.11.001
28. Lenting PJ, Westein E, Terraube V, Ribba AS, Huizinga EG, Meyer D, de Groot PG, Denis CV. An experimental model to study the *in vivo* survival of von Willebrand factor. Basic aspects and application to the R1205H mutation. *J Biol Chem.* 2004;279:12102–12109. doi: 10.1074/jbc.M310436200
29. Obert B, Tout H, Veyradier A, Fressinaud E, Meyer D, Girma JP. Estimation of the von Willebrand factor-cleaving protease in plasma using monoclonal antibodies to vWF. *Thromb Haemost.* 1999;82:1382–1385.
30. Powers WJ, Rabinstein AA, Ackerson T, Adeoye OM, Bambakidis NC, Becker K, Biller J, Brown M, Demaerschalk BM, Hoh B, et al; American Heart Association Stroke Council. 2018 Guidelines for the early management of patients with acute ischemic stroke: a guideline for healthcare professionals from the American Heart Association/American Stroke Association. *Stroke.* 2018;49:e46–e110. doi: 10.1161/STR.0000000000000158
31. Matsuzawa T, Nomura M, Unno T. Clinical pathology reference ranges of laboratory animals. Working group II, nonclinical safety evaluation subcommittee of the Japan pharmaceutical manufacturers association. *J Vet Med Sci.* 1993;55:351–362. doi: 10.1292/jvms.55.351
32. Dorahy DJ, Thorne RF, Fecondo JV, Burns GF. Stimulation of platelet activation and aggregation by a carboxyl-terminal peptide from thrombospondin binding to the integrin-associated protein receptor. *J Biol Chem.* 1997;272:1323–1330. doi: 10.1074/jbc.272.2.1323
33. Roberts W, Magwenzi S, Aburima A, Naseem KM. Thrombospondin-1 induces platelet activation through CD36-dependent inhibition of the cAMP/protein kinase A signaling cascade. *Blood.* 2010;116:4297–4306. doi: 10.1182/blood-2010-01-265561
34. Kuijpers MJ, de Witt S, Nergiz-Unal R, van Kruchten R, Korporaal SJ, Verhamme P, Febbraio M, Tjwa M, Voshol PJ, Hoylaerts MF, et al. Supporting roles of platelet thrombospondin-1 and CD36 in thrombus formation on collagen. *Arterioscler Thromb Vasc Biol.* 2014;34:1187–1192. doi: 10.1161/ATVBAHA.113.302917
35. Aburima A, Berger M, Spurgeon BE, Webb BA, Wraith KS, Febbraio M, Poole AW, Naseem KM. Thrombospondin-1 promotes haemostasis through modulation of cAMP signalling in blood platelets. *Blood.* 2020;blood.2020005382. doi: 10.1182/blood.2020005382
36. Marqus S, Pirogova E, Piva TJ. Evaluation of the use of therapeutic peptides for cancer treatment. *J Biomed Sci.* 2017;24:21. doi: 10.1186/s12929-017-0328-x
37. Jarvis GE, Atkinson BT, Snell DC, Watson SP. Distinct roles of GPVI and integrin alpha(2)beta(1) in platelet shape change and aggregation induced by different collagens. *Br J Pharmacol.* 2002;137:107–117. doi: 10.1038/sj.bjp.0704834
38. Moroi M, Jung SM, Okuma M, Shinmyozu K. A patient with platelets deficient in glycoprotein VI that lack both collagen-induced aggregation and adhesion. *J Clin Invest.* 1989;84:1440–1445. doi: 10.1172/JCI114318
39. Roberts DD, Miller TW, Rogers NM, Yao M, Isenberg JS. The matricellular protein thrombospondin-1 globally regulates cardiovascular function and responses to stress via CD47. *Matrix Biol.* 2012;31:162–169. doi: 10.1016/j.matbio.2012.01.005
40. Rogers NM, Seeger F, Garcin ED, Roberts DD, Isenberg JS. Regulation of soluble guanylate cyclase by matricellular thrombospondins: implications for blood flow. *Front Physiol.* 2014;5:134. doi: 10.3389/fphys.2014.00134
41. Dixit VM, Haverstick DM, O'Rourke KM, Hennessy SW, Grant GA, Santoro SA, Frazier WA. A monoclonal antibody against human thrombospondin inhibits platelet aggregation. *Proc Natl Acad Sci U S A.* 1985;82:3472–3476. doi: 10.1073/pnas.82.10.3472
42. Fujimoto TT, Katsutani S, Shimomura T, Fujimura K. Thrombospondin-bound integrin-associated protein (CD47) physically and functionally modifies integrin alphaIIbbeta3 by its extracellular domain. *J Biol Chem.* 2003;278:26655–26665. doi: 10.1074/jbc.M302194200
43. Savage B, Saldívar E, Ruggeri ZM. Initiation of platelet adhesion by arrest onto fibrinogen or translocation on von Willebrand factor. *Cell.* 1996;84:289–297. doi: 10.1016/s0092-8674(00)80983-6
44. Pimanda JE, Ganderton T, Maekawa A, Yap CL, Lawler J, Kershaw G, Chesterman CN, Hogg PJ. Role of thrombospondin-1 in control of von Willebrand factor multimer size in mice. *J Biol Chem.* 2004;279:21439–21448. doi: 10.1074/jbc.M313560200

45. Cooley BC. Murine models of thrombosis. *Thromb Res*. 2012;129 Suppl 2:S62–S64. doi: 10.1016/j.thromres.2012.02.036
46. Day SM, Reeve JL, Myers DD, Fay WP. Murine thrombosis models. *Thromb Haemost*. 2004;92:486–494.
47. Eckly A, Hechler B, Freund M, Zerr M, Cazenave JP, Lanza F, Mangin PH, Gachet C. Mechanisms underlying FeCl3-induced arterial thrombosis. *J Thromb Haemost*. 2011;9:779–789. doi: 10.1111/j.1538-7836.2011.04218.x
48. Lawler J, Sunday M, Thibert V, Duquette M, George EL, Rayburn H, Hynes RO. Thrombospondin-1 is required for normal murine pulmonary homeostasis and its absence causes pneumonia. *J Clin Invest*. 1998;101:982–992. doi: 10.1172/JCI1684
49. Qi ZY, Liu X, Bai YN, Ge JB. Alginate oligosaccharide inhibits platelet activation with minimal impact on bleeding time. *Cardiol Plus*. 2020;5:42–50.
50. Raife TJ, Cao W, Atkinson BS, Bedell B, Montgomery RR, Lentz SR, Johnson GF, Zheng XL. Leukocyte proteases cleave von Willebrand factor at or near the ADAMTS13 cleavage site. *Blood*. 2009;114:1666–1674. doi: 10.1182/blood-2009-01-195461
51. Tersteeg C, de Maat S, De Meyer SF, Smeets MW, Barendrecht AD, Roest M, Pasterkamp G, Fijnheer R, Vanhoorelbeke K, de Groot PG, et al. Plasmin cleavage of von Willebrand factor as an emergency bypass for ADAMTS13 deficiency in thrombotic microangiopathy. *Circulation*. 2014;129:1320–1331. doi: 10.1161/CIRCULATIONAHA.113.006727
52. Wang A, Liu F, Dong N, Ma Z, Zhang J, Su J, Zhao Y, Ruan C. Thrombospondin-1 and ADAMTS13 competitively bind to VWF A2 and A3 domains *in vitro*. *Thromb Res*. 2010;126:e260–e265. doi: 10.1016/j.thromres.2010.07.009
53. McFadyen JD, Schaff M, Peter K. Current and future antiplatelet therapies: emphasis on preserving haemostasis. *Nat Rev Cardiol*. 2018;15:181–191. doi: 10.1038/nrcardio.2017.206